Calhoun: The NPS Institutional Archive

DSpace Repository

Theses and Dissertations | 1. Thesis and Dissertation Collection, all items

1989-06

A numerical study of topographically steered flows in the Fram Strait.

McShane, David W.

Monterey, California. Naval Postgraduate School

http://hdl.handle.net/10945/26115

This publication is a work of the U.S. Government as defined in Title 17, United States Code, Section 101. Copyright protection is not available for this work in the United States.

Downloaded from NPS Archive: Calhoun

http://www.nps.edu/library

Calhoun is the Naval Postgraduate School's public access digital repository for research materials and institutional publications created by the NPS community. Calhoun is named for Professor of Mathematics Guy K. Calhoun, NPS's first appointed -- and published -- scholarly author.

Dudley Knox Library / Naval Postgraduate School
411 Dyer Road / 1 University Circle
Monterey, California USA 93943

D DLEY KNOX LIBRARY
NAVAL POSTGRADUATE SCHOOL
MONTEREY, CALIFORNIA 93943-5002

NAVAL POSTGRADUATE SCHOOL
Monterey, California

THESIS

A NUMERICAL STUDY OF TOPOGRAPHICALLY STEERED FLOWS IN THE FRAM STRAIT

by

David W. McShane

June 1989

Thesis Advisor David C. Smith IV

Approved for public release; distribution is unlimited.

T244008

REPORT DOCUMENTATION PAGE

Report Security Classification Unclassified		1b Restrictive Markings	
Security Classification Authority		3 Distribution/Availability of Report	
Declassification Downgrading Schedule		Approved for public release; distribution is unlimited.	
Performing Organization Report Number(s)		5 Monitoring Organization Report Number(s)	
Name of Performing Organization aval Postgraduate School	6b Office Symbol *(if applicable)* 35	7a Name of Monitoring Organization Naval Postgraduate School	
Address *(city, state, and ZIP code)* onterey, CA 93943-5000		7b Address *(city, state, and ZIP code)* Monterey, CA 93943-5000	
Name of Funding Sponsoring Organization	8b Office Symbol *(if applicable)*	9 Procurement Instrument Identification Number	
Address *(city, state, and ZIP code)*		10 Source of Funding Numbers	
		Program Element No	Project No / Task No / Work Unit Accession No

Title *(include security classification)* A NUMERICAL STUDY OF TOPOGRAPHICALLY STEERED FLOWS IN THE RAM STRAIT

Personal Author(s) David W. McShane

a Type of Report aster's Thesis	13b Time Covered From To	14 Date of Report *(year, monih, day)* June 1989	15 Page Count 53

Supplementary Notation The views expressed in this thesis are those of the author and do not reflect the official policy or po-ion of the Department of Defense or the U.S. Government.

Cosati Codes			18 Subject Terms *(continue on reverse if necessary and identify by block number)*
eld	Group	Subgroup	Fram Strait, East Greenland Current, West Spitzbergen Current, Return Atlantic Current, two-layered, primitive equation,

Abstract *(continue on reverse if necessary and identify by block number)*

The Fram Strait is a region of complex circulation and intense dynamical activity. Its general circulation is largely influ-ced by the East Greenland Current (EGC), the associated Marginal Ice Zone jet, the West Spitzbergen Current (WSC) and e topography of the region. The general circulation was studied using a two-layered numerical model. Forcing of the model as done by varying: the inflow and outflow velocity; the port locations and boundary conditions; and by adjustment of pography. Representative topography of the Fram Strait was modeled in the lower layer. Results indicate that the model sensitive to EGC width and its proximity to the western boundary; and that in the absence of EGC flow, the Return lantic Current does not exist. Investigation of model sensitivity to WSC inflow vertical shear led to the conclusion that hen the WSC inflow is 10 cm/sec in the upper layer and 5 cm/sec in the lower layer, a boundary trapped component of the SC is generated.

Distribution Availability of Abstract unclassified unlimited ☐ same as report ☐ DTIC users	21 Abstract Security Classification Unclassified	
a Name of Responsible Individual avid C. Smith IV	22b Telephone *(include Area code)* (408) 646-3350	22c Office Symbol 68Si

) FORM 1473,84 MAR 83 APR edition may be used until exhausted
All other editions are obsolete

security classification of this page

Unclassified

Approved for public release; distribution is unlimited.

A Numerical Study of Topographically
Steered Flows in the Fram Strait

by

David W. McShane
Lieutenant Commander, United States Navy
B.S., Auburn University, 1979
MBA, National University, 1985

Submitted in partial fulfillment of the
requirements for the degree of

MASTER OF SCIENCE IN METEOROLOGY AND OCEANOGRAPHY

from the

NAVAL POSTGRADUATE SCHOOL
June 1989

ABSTRACT

The Fram Strait is a region of complex circulation and intense dynamical activity. Its general circulation is largely influenced by the East Greenland Current (EGC), the associated Marginal Ice Zone jet, the West Spitzbergen Current (WSC) and the topography of the region. The general circulation was studied using a two-layered numerical model. Forcing of the model was done by varying: the inflow and outflow velocity; the port locations and boundary conditions; and by adjustment of topography. Representative topography of the Fram Strait was modeled in the lower layer. Results indicate that the model is sensitive to EGC width and its proximity to the western boundary; and that in the absence of EGC flow, the Return Atlantic Current does not exist. Investigation of model sensitivity to WSC inflow vertical shear led to the conclusion that when the WSC inflow is 10 cm/sec in the upper layer and 5 cm/sec in the lower layer, a boundary trapped component of the WSC is generated.

1 Ra513
M26877
C.1

TABLE OF CONTENTS

NAVAL POSTGRADUATE SCHOOL
MONTEREY, CALIFORNIA 93943-5002

LIST OF TABLES

LIST OF FIGURES

I. INTRODUCTION

A. THE FRAM STRAIT REGION

The area between East Greenland and Svalbard is considered to be of extreme importance since it provides the primary connection between the North Atlantic Ocean and the Arctic Ocean. The complex circulation and intense dynamical activity has for many years been of great interest, both from a military and scientific standpoint. Figure 1, from Paquette *et al.*, (1985), shows the general circulation and topography of the region. The East Greenland Current (EGC) and the associated frontal jet (see figure 1), sometimes referred to as the East Greenland Polar Front, moves cold low-salinity water from the Arctic basin to the south along the Greenland coast. The West Spitzbergen Current (WSC) (see figure 1) carries warm saline water to the north, west of Svalbard. According to Gascard *et al.*, (1988), the West Spitzbergen Current generally flows toward the northwest along the Yermak Plateau (see figure 3) west of Svalbard and splits into several branches in the vicinity of 78° - 79° N with a branch continuing to the northeast and the others turning west, one being associated with the Molloy Deep (see figure 1) area (surrounded by the Spitzbergen Fracture Zone) on the south, and the other associated with the Hovgaard Fracture Zone (see figure 3). Much of the definition of the circulation in the region has come from observations using shipboard sensors, the Marginal Ice Zone Experiment (MIZEX) data sets, drifting buoys, and satellite imagery. It is generally thought that the West Spitzbergen Current, the jet-like East Greenland Current, and the Return Atlantic Current (RAC) (see figure 1) provide the basis for the Fram Strait circulation. This circulation generally follows the topography, Foldvik *et al.*, (1988), Gascard *et al.*, (1988), Paquette *et al.*, (1985), Quadfasel *et al.*, (1987).

Figure 2 is from Aagaard *et al.*, (1988), and shows the actual bathymetry of the region in greater detail. A current meter was positioned at FS-9B (see figure 2) and the velocities obtained from FS-9B were compared with model current velocities (in a later section).

B. THE OBSERVED VELOCITY AND TRANSPORT WITHIN THE FRAM STRAIT REGION

The East Greenland Current is considered to be a western boundary current flowing generally southward with its strongest flow over the continental slope. The East Greenland Current has been observed to be baroclinic in nature, with currents typically

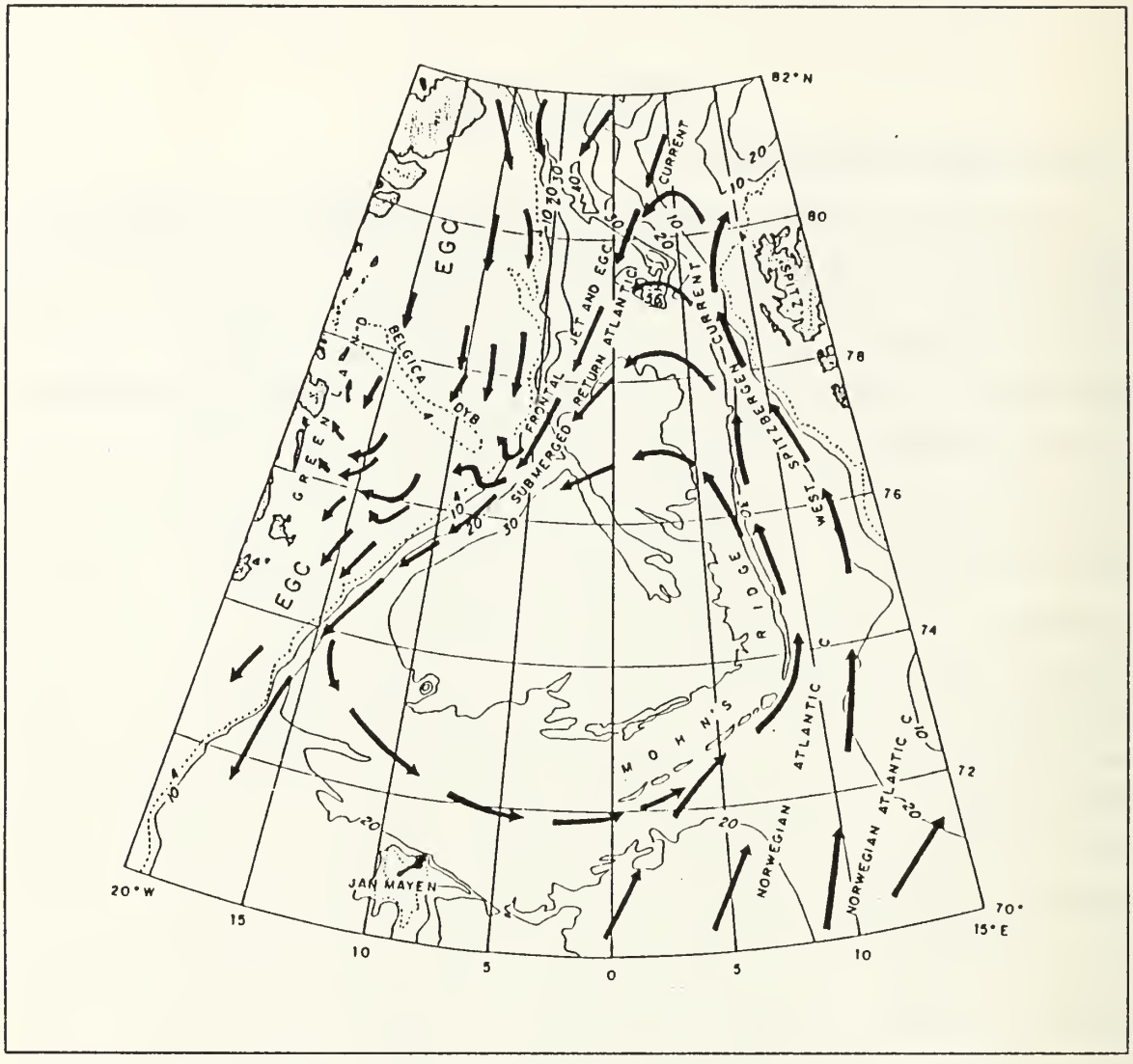

Figure 1. Bathymetry and Currents in the Fram Strait (from Paquette et al., (1985)): Depth labels are in hundreds of meters. The 5600 meter depression at 79° North is the Molloy Deep.

computed at 20-30 cm/sec, in the upper layer (Foldvik *et al.*, (1988)). Velocities as high as 1 m/sec have been reported by Paquette *et al.*, 1985. This current produces a characteristic baroclinic transport of approximately 3 Sverdrups (Sv) over the upper few hundred meters.

There is a predominant cyclonic circulation within the Greenland Sea, this being caused at least in part by the wind stress curl and the guiding of flow along the topog-

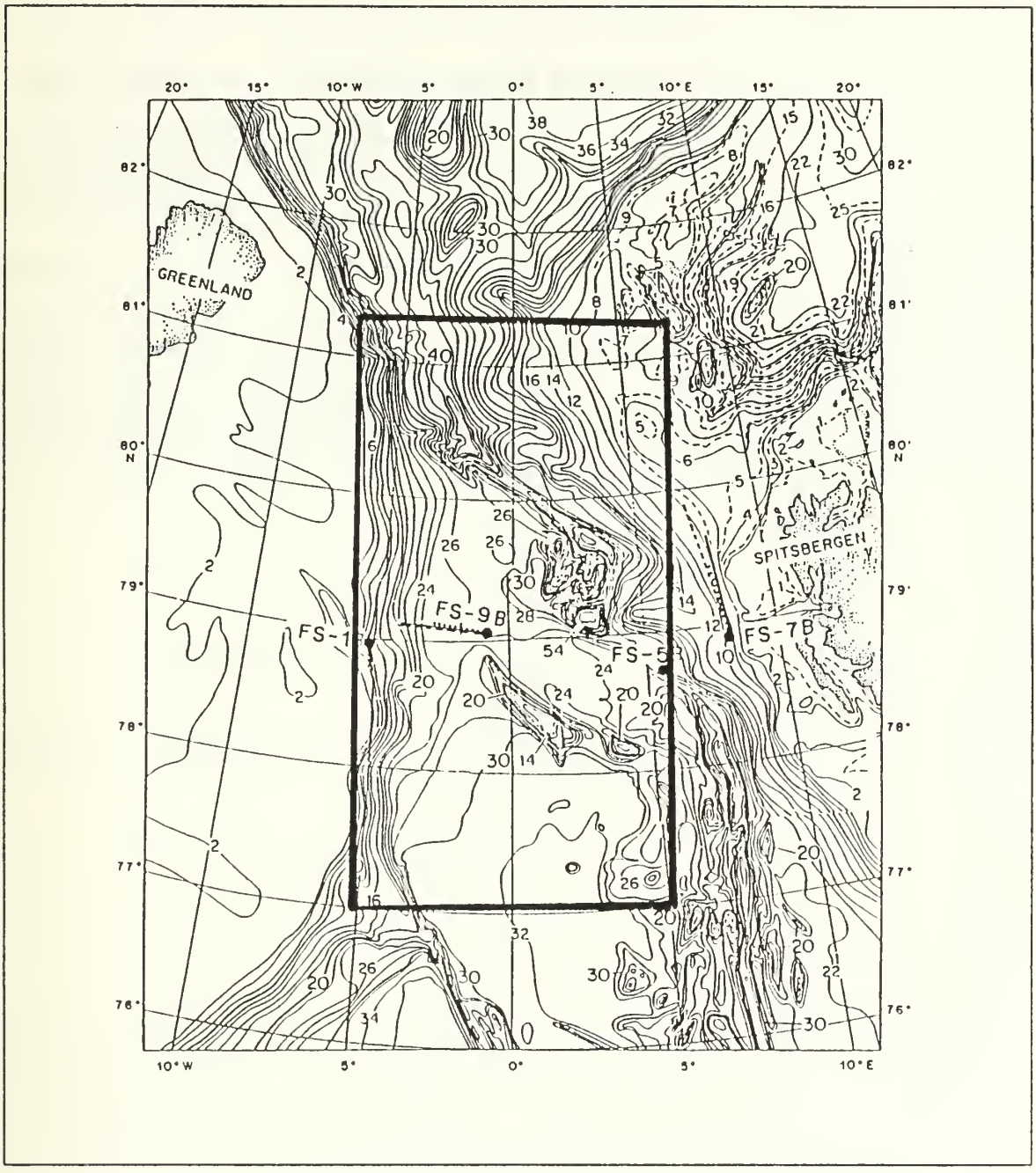

Figure 2. Fram Strait Bathymetry (from Aagaard et al., (1988)): Depth labels are in hundreds of meters. Note position of FS-9B. The rectangle indicates the numerical model domain (522 km by 395 km) used in this study.

raphy of the region west of Svalbard (Quadfasel *et al.*, (1987)). The northern portion of this cyclonic gyre forms the Return Atlantic Circulation (RAC). Current speeds of up to 40 cm/sec have been observed in the West Spitzbergen Current, with a mean transport value of about 3 Sv (varied from 0 to 9 Sv), Aagaard (1982), Hanzlick (1983) Gascard *et al.*, (1988). Aagaard *et al.*, (1988) compiled current meter data from the Fram Strait, and data from their FS-9B current meter (see figure 2.) will be compared with model currents in a later section.

C. PURPOSE OF THIS STUDY

The objective of this study is to examine how barotropic and baroclinic current flows interact with bathymetry to produce the observed Fram Strait circulation. This is accomplished through the use of a nonlinear, two-layer, regional numerical model with currents over idealized Fram Strait topography.

II. NUMERICAL SIMULATION OF THE FRAM STRAIT REGION

A. THE NUMERICAL MODEL

1. Model Equations

The circulation within the Fram Strait is modeled using a two layer, semi-implicit, primitive equation, numerical scheme. The scheme was initially used by Hurlburt (1974) in ocean circulation studies and has been employed numerous times (Hurlburt and Thompson (1980, 1982); Smith and O'Brien (1983); and Smith and Davis (1989)). Linear test cases have been run for comparison with linear analytic solutions to show model validity (Smith and Reid, 1982). Motion within each layer is governed by a momentum equation (2.1) and by a continuity equation (2.2).

$$\frac{\partial V_i}{\partial t} + (\nabla \cdot V_i + V_i \cdot \nabla)v_i + \hat{k} \times fV_i = - h_i \nabla P_i - B_h \nabla^4 V_i \qquad (Eqn 2.1)$$

$$\frac{\partial h_i}{\partial t} + \nabla \cdot V_i = 0 \qquad (Eqn 2.2)$$

The EGC jet (when included as a initial condition) is defined:

$$h_1(x,y) = \overline{H}_1 - (A_I + A_S)\left[1 - e^{\frac{-(y-y_0)^2}{2L_j^2}}\right] \quad (y \geq y_0) \qquad (Eqn 2.3)$$

$$h_2(x,y) = \overline{H}_2 \qquad + A_I\left[1 - e^{\frac{-(y-y_0)^2}{2L_j^2}}\right] \quad (y \geq y_0) \qquad (Eqn 2.4)$$

Subscript i denotes upper (i = 1) or lower (i = 2) layer. V_1 and V_2 are depth integrated transports in each layer. Upper layer mean thickness ($\overline{H}_1$) is chosen to be 200 m. The lower layer mean thickness ($\overline{H}_2$) is 5400 m. The first internal Rossby radius of deformation (R_d) associated with this layer thickness distribution is approximately 14 km. The Coriolis parameter f is taken to be a constant. A_I and A_S are interface and surface distortion amplitudes (= 75.0 meters and 0.2 meters respectively). L_j is the e-folding width scale for the jet, and y_0 is the eastern edge of the jet located 67 km from the western boundary. The amplitudes A_I, A_S were chosen to give a maximum jet velocity (v_{max}) of approximately 40 cm/s in the upper layer and 10 cm/s in the lower layer in all experiments.

Variables and notation are defined in the appendix. The fluid in both layers is assumed to be hydrostatic and Boussinesq, and the fluid density in each layer is constant. The effects of winds, ice, tides, thermodynamics and thermohaline mixing are not included.

2. Model Domain

A rectangular region (521.7 km x 395.0 km) was divided into 4.7 km by 5.0 km rectangles to form the grid for the numerical model finite differencing. The grid was oriented to have the Molloy Deep and nearby Hovgaard fracture zone near the center, at 79.40° N, 1.53° E.

Topography is included by applying a smoothed field of gridded bathymetry into the model for each corner of the 4.7 km by 5.0 km rectangles. Due to a model constraint that the layer interface cannot intersect the free surface or the topography, the shallowest topography was 600 meters. Because of this constraint, shallow topography and nearshore processes could not be included within this model. Figure 3 shows the topography used within the model, while Figure 2 shows the actual Fram Strait topography. Note that the major features of the topography like the Molloy Deep, Yermak Plateau, East Greenland continental slope, and fracture zones are preserved. Small scale features, such as several seamounts in the Molloy Deep, which are thought to be important for the circulation there (Bourke *et al.*, 1987), are not resolved.

3. Boundary Conditions

Two separate and distinct boundary conditions were used in this model. For the east and west sides of the Fram Strait a no-slip boundary condition was used. For the open (north and south sides) portions of the Fram Strait a prescribed inflow and outflow boundary condition was set to represent the West Spitzbergen current and the East Greenland Current. The inflow velocity was ramped up to its maximum value in approximately 5 to 6 days in cases which are boundary forced only. In cases in which an EGC jet extends across the domain in the initial condition, the EGC inflow condition is maintained constant in time. The lateral distribution of the inflow is Gaussian with an e-folding scale of 20 km. For the EGC, the Gaussian function is centered in the inflow port; for the WSC, the jet is centered on grid point 10. An open outflow radiation boundary condition (Camerlengo and O'Brien (1980)) was specified on the north and south boundaries anywhere that did not have inflow. Inflow and outflow specifications are described in greater detail in the experiments section.

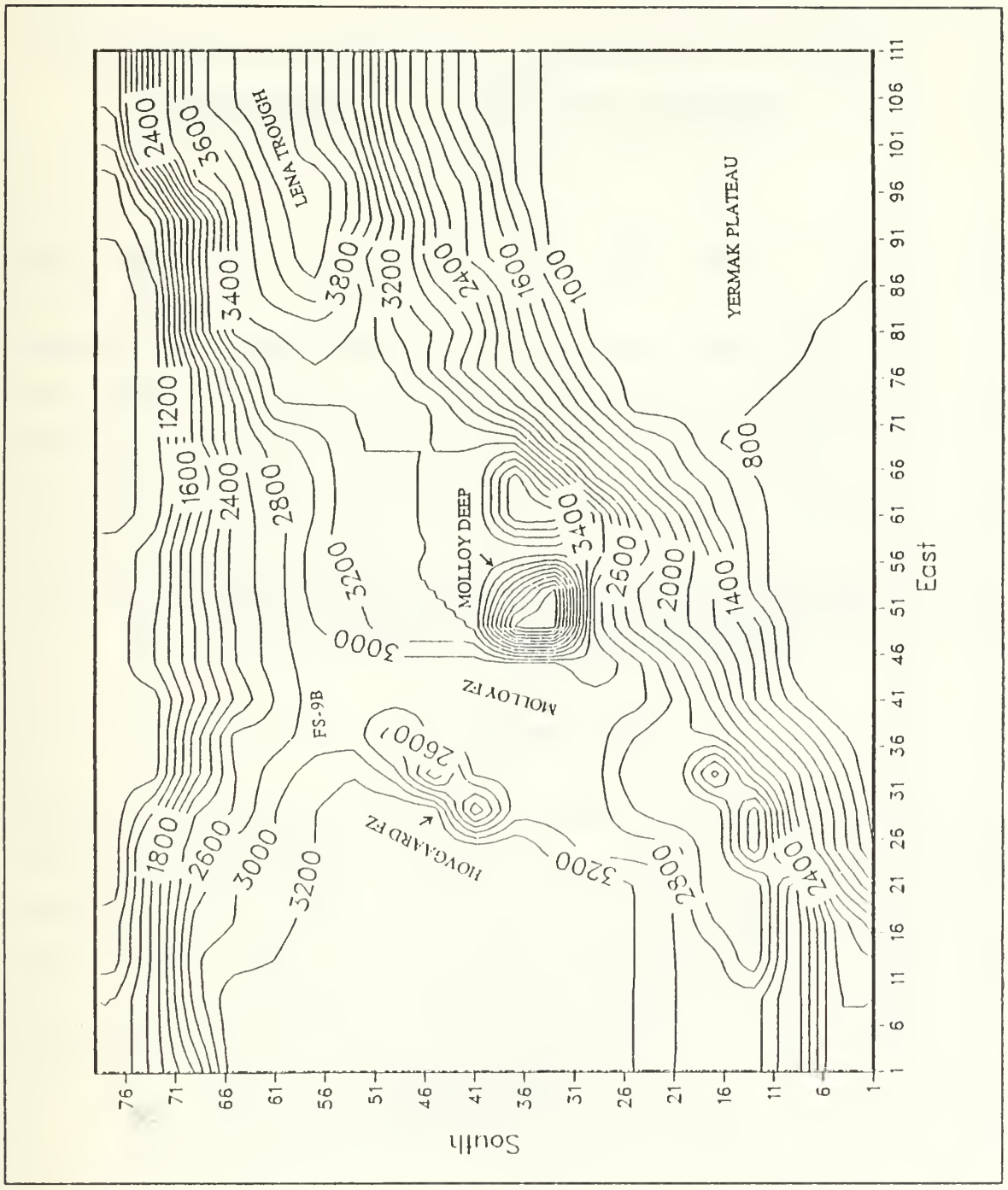

Figure 3. Modeled Fram Strait Topography: Depth contours are indicated in meters. Locations of inflow boundary forcing are specified in terms of grid points on the north and south boundaries.

4. Preliminary Considerations

For a linear, inviscid, two-layer fluid, fluid particles can be shown to conserve potential vorticity

$$Q_i = \frac{f + \zeta_i}{h_i}$$

where ζ_i is relative vorticity ($= \frac{\partial v_i}{\partial x} - \frac{\partial u_i}{\partial y}$) in each layer and h_i is instantaneous layer thickness.

Figure 4 shows initial upper and lower layer potential vorticity for the EGC jet initialized case at day zero. The jet extends along the whole western boundary. Considering the lower layer potential vorticity first, it is obvious that the major contributions to Q_2 are the depth variations associated with bathymetry. Contrast this figure with figure 3 (topography). Thus, if frictional or nonlinear effects are small, fluid particles in the lower layer will follow contours of bathymetry. There may be different circulation patterns possible depending on where a fluid particle enters the domain. The Rossby number for the lower layer of the initial EGC:

$$\frac{u_2}{fL} = \frac{.1}{(f \times 20{,}000)} = .03$$

indicates that nonlinear effects are unlikely to overcome the strong topographic steering. Likewise, frictional effects are small in the momentum balance (equation number 2.1) by choice of B_h. Transient vorticity-conserving wave motions, such as topographic Rossby waves, can however also exist in which cross isobath changes in vorticity associated with changes in h_2 are balanced by relative vorticity changes ζ_2.

In the upper layer, the jet's relative vorticity dominates the potential vorticity Q_1. In contrast to the lower layer, the Rossby number for the upper layer

$$\frac{u_1}{fL} = .14$$

indicates that nonlinear effects may not be negligible.

Associated with lateral and vertical shears in the initial conditions, conditions for barotropic and baroclinic instability may be met. It is a goal of this research to examine topographically steered flows in the Fram Strait region for stable flows before the

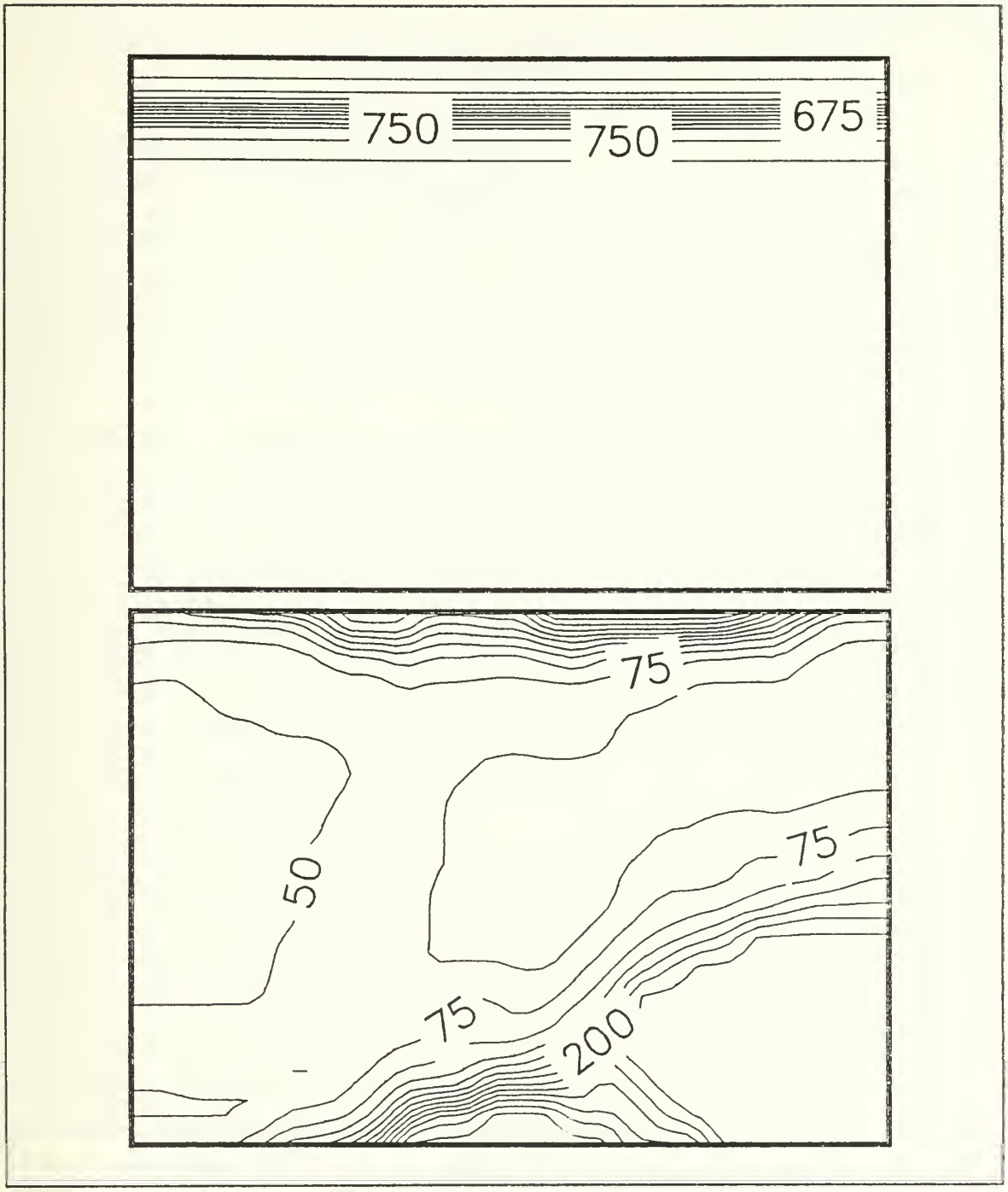

Figure 4. Upper and Lower Layer Potential Vorticity: North is to the right in both charts. Upper and lower layer contour intervals are 25 x 10^{-6} sec^{-1}.

more complex problem of unstable flows in the region can be examined. The time scale for these instabilities is likely longer than the duration of the experiments presented here.

III. EXPERIMENTS

A. PURPOSE OF THE EXPERIMENTS

The purpose of the following experiments is to understand the factors that contribute to the general circulation of the Fram Strait. A key objective of this study is to determine the effect topography has on the circulation, and this is reasonably well demonstrated with the model. Additionally, questions of baroclinic versus barotropic inflow forcing are explored as well as initialization of the East Greenland Current with a jet.

Output from the model is in the form of charts of upper and lower layer velocities, and charts of upper and lower layer potential vorticity. All simulations were run for 10 days. This period was adequate for topographically steered flows to evolve, but did not allow the flow to evolve to the point of demonstrating mesoscale instabilities. To aid in comparing modeled output with observed data, the current was sampled at a specific location within the model domain and then compared with *in situ* current meter data from Aagaard *et al.*, (1988). The model current is measured at grid position (36, 56), (see figure 3 for location) within the model domain so that model output velocity at this location can be compared with FS-9B velocity data.

B. PRELIMINARY EXPERIMENTS

Table 1 lists the preliminary experiments and parameters that were varied. Experiments No. 1 through 3 were EGC boundary forced (inflow allowed only at a specified location and outflow everywhere else on the boundary), and Experiments No. 4 through 6 were EGC jet initialized (equations 2.3 and 2.4). All of the preliminary experiments were run utilizing the modeled Fram Strait topography of figure 3. All velocity fields are displayed at 10 days. Shears, such as 40 cm/sec in the upper layer and 10 cm/sec in the lower layer will be indicated by a shorthand notation of 40/10 cm/sec, or as 40 10 cm/sec in the upper and lower layers respectively. This form of notation will be used in figure captions as well as text.

Each numerical simulation was run with a variation of one parameter. Of interest was how the East Greenland Current (EGC) and the West Spitzbergen Current (WSC) interact with the region's topography to produce the observed topographically steered flows. In this section the results of the preliminary experiments are described.

1. **Experiment No. 1 (No Jet Initialization, WSC shear 10/10 cm/sec)**

In this simulation there was no jet initialization of the EGC, and the WSC was initially barotropic with a velocity of 10 cm/sec in each layer. While a portion of EGC evolves along the western boundary, a substantial portion is steered down the Lena trough. Return Atlantic Current flow exists via the forcing of the WSC and the joining of EGC water flowing down the Lena trough. Large velocities are seen in the Hovgaard Fracture Zone associated with convergent effects of topography. A weak along boundary current component of the EGC is observed in the upper layer. No northward along boundary flow of WSC is observed. An anticyclonic feature is seen over the Yermak plateau in both the upper and lower layers and will be discussed later in this section. The velocity fields are depicted in figure 5.

Table 1. PRELIMINARY VARIATION OF MODEL PARAMETERS

Experiment No.	EGC Inflow Location on Northern Boundary	EGC v_1/v_2 (cm/sec)	WSC Inflow Location on Southern Boundary	WSC v_1/v_2 (cm/sec)	Jet (yes/no)
1	55-75	40 10	5-35	10 10	no
2	55-75	40 10	5-35	10 5	no
3	55-75	40 10	5-35	10 1	no
4	55-75	40 10	5-35	10 10	yes
5	55-75	40 10	5-35	10 5	yes
6	55-75	40 10	5-35	10 1	yes

2. **Experiment No. 2 (No Jet Initialization, WSC shear 10/5 cm/sec)**

The WSC inflow vertical shear was changed to 10 5 cm/sec in the upper and lower layers respectively for this simulation. RAC exists via a westward flowing branch of the WSC in both the upper and lower layers. The formation of along boundary flow in both the WSC and EGC regions is seen in the upper layer and is suggestive of an eastern branch of the WSC and an along isobath jet-like structure to the EGC. The velocity fields are depicted in figure 6.

3. **Experiment No. 3 (No Jet Initialization, WSC shear 10/1 cm/sec)**

In this simulation, the WSC inflow shear was again increased. The along boundary component of the EGC is seen in the upper layer. There appears to be no coupling of a WSC component with the southward arctic flow from the Lena trough in

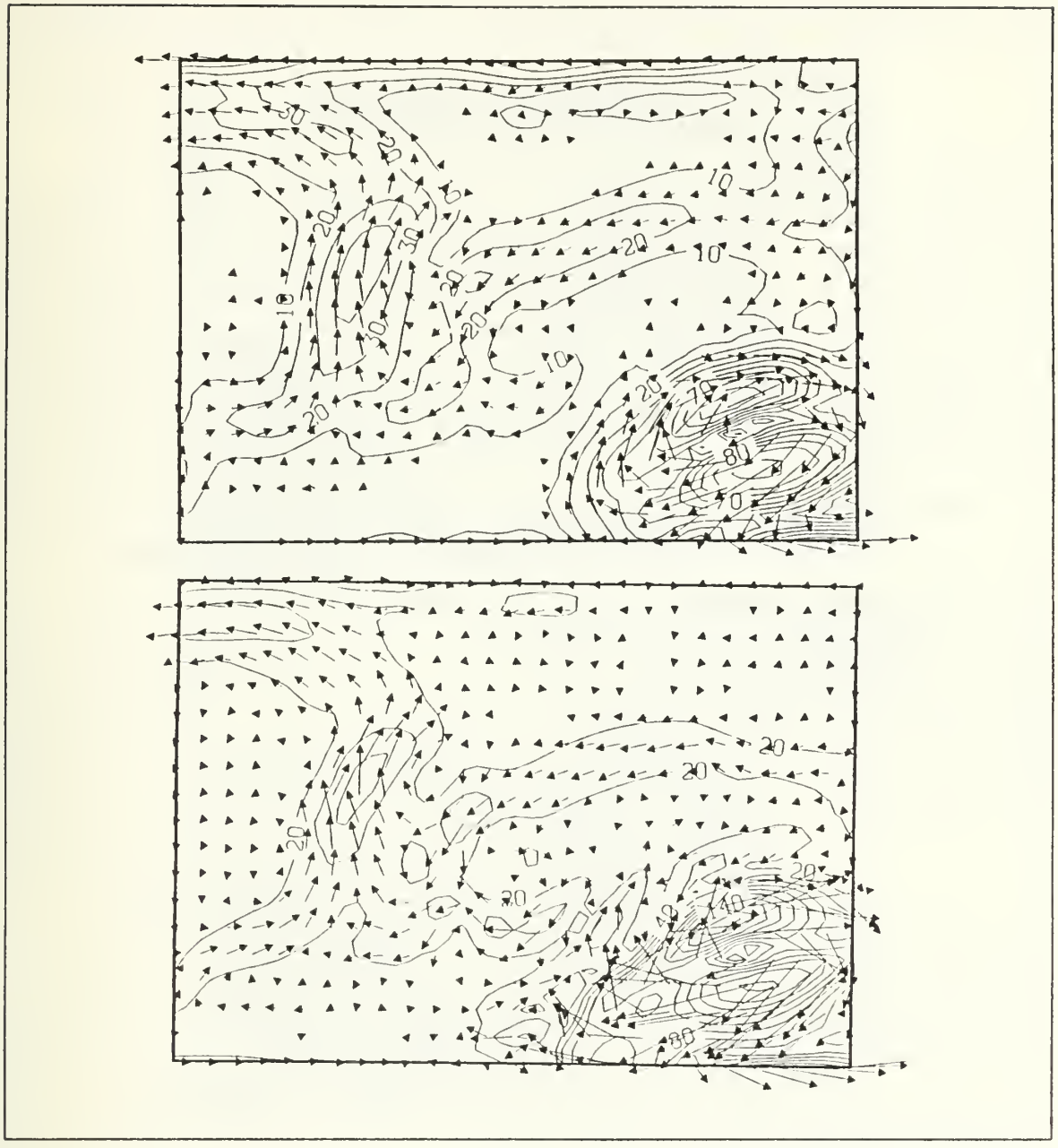

Figure 5. Experiment No. 1 (No Jet Initialization, WSC shear 10/10 cm/sec): The upper and lower figures represent upper and lower layer velocity fields respectively for Experiment No. 1. North is to the right in each figure and each figure represents a 522 km by 395 km area. Contour intervals are 10 and 20 cm/sec for the upper and lower layer respectively.

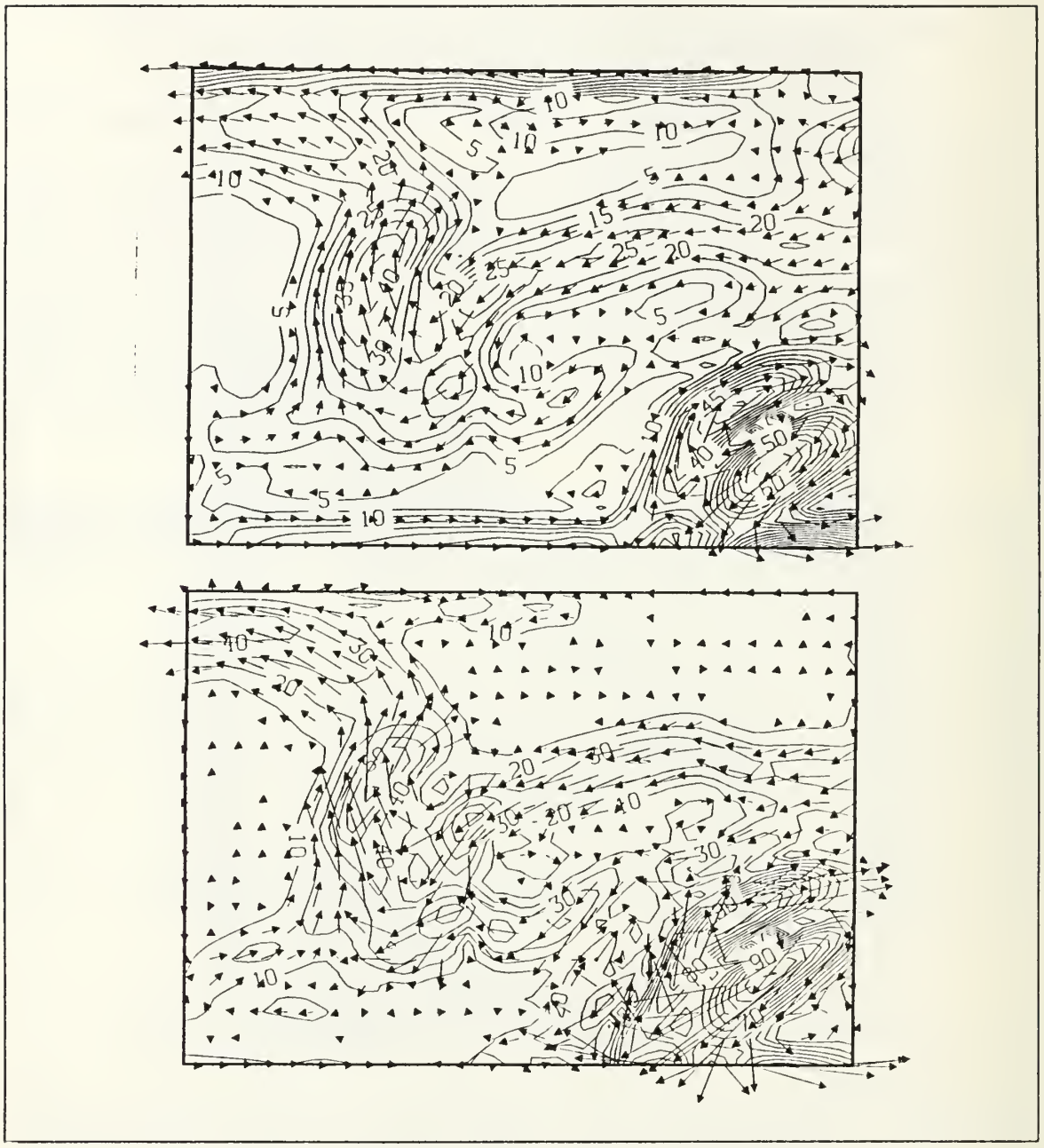

Figure 6. Experiment No. 2 (No Jet Initialization, WSC shear 10/5 cm/sec): The upper and lower figures represent the upper and lower layer velocity fields respectively for Experiment No. 2. North is to the right and each figure represents a 522 km by 395 km area. Contour intervals are 5 and 10 cm/sec for the upper and lower layers respectively.

the upper layer, but the WSC appears to connect with the RAC in the lower layer. The upper WSC has formed an along boundary northward flow pattern. The velocity fields are depicted in figure 7.

4. Experiment No. 4 (Jet Initialization, WSC shear 10/10 cm/sec)

This simulation was initialized with an EGC jet across the domain (along western boundary). Its orientation and location relative to the East Greenland boundary is shown in figure 4 (upper). Initially, the jet's upper layer velocity was 40 cm/s and lower layer velocity was 10 cm/s. The EGC inflow was boundary forced with 40/10 cm/s in the upper and lower layers respectively. The WSC was boundary forced with 10/10 cm/s in the upper and lower layers. On day 10, along boundary EGC exists in the upper layer. The RAC is not well organized in the upper layer in the region of the juncture with the EGC outflow, but does exist. A weak, narrow, along boundary component of WSC is seen in both the upper and lower layers. The velocity fields are depicted in figure 8.

5. Experiment No. 5 (Jet Initialization, WSC shear 10/5 cm/sec)

As in the previous experiment an EGC jet was initialized, with velocities of 40 cm/s upper layer and 10 cm s lower layer. Weak EGC along boundary flow exists in both the upper and lower layers, but appears more organized in the upper layer. WSC induced RAC exists. The westward flowing RAC is not well organized near its junction with the EGC in the upper layer, but the lower layer appears more organized. The along boundary component of the WSC is well formed in the upper layer, but very weak if at all in the lower layer. The velocity fields are depicted in figure 9.

6. Experiment No. 6 (Jet Initialization, WSC shear 10/1 cm/sec)

This simulation was initialized with an EGC jet across the domain in the upper and lower layers. Little along boundary continuous deep EGC is seen with the exception of a small amount near the southern outflow region. Instead, cross isobath topographic Rossby wave variability extends along much of the slope. WSC induced RAC does not exist in the upper layer. The WSC component is totally boundary trapped in the upper layer. The lower layer shows RAC to the west. There is no along boundary component of WSC in the lower layer. The velocity fields are depicted in figure 10.

Preliminary Experiments No. 1 through 6 all exhibit an anticyclonic vortex or vortices in the vicinity of the Yermak plateau. The Yermak plateau is the shallowest region within the model domain with a-mean depth of 600-1200 meters. The boundary forcing of the WSC inflow at the 2400 meters to 3200 meters isobath (southern boundary) causes along isobath flow toward the Yermak plateau. To exit the open boundary in shallow water on the Yermak Plateau, fluid columns are forced upslope. This flow is

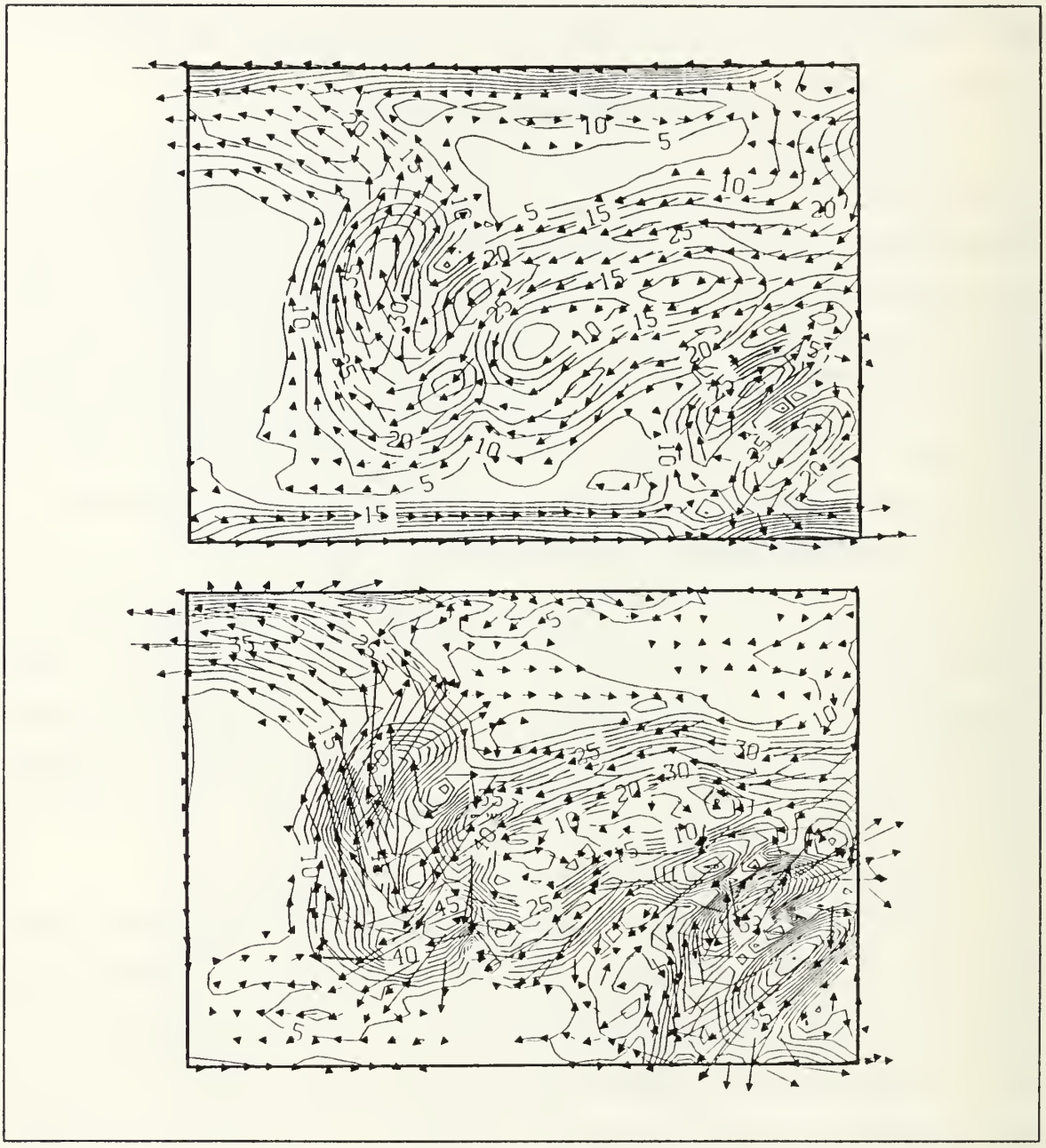

Figure 7. Experiment No. 3 (No Jet Initialization, WSC shear 10/1 cm/sec): The upper and lower figures represent the upper and lower velocity fields respectively for Experiment No. 3. North is to the right in each figure and each figure represents a 522 km by 395 km area. Contour intervals are 5 cm/sec for both the upper and lower layers.

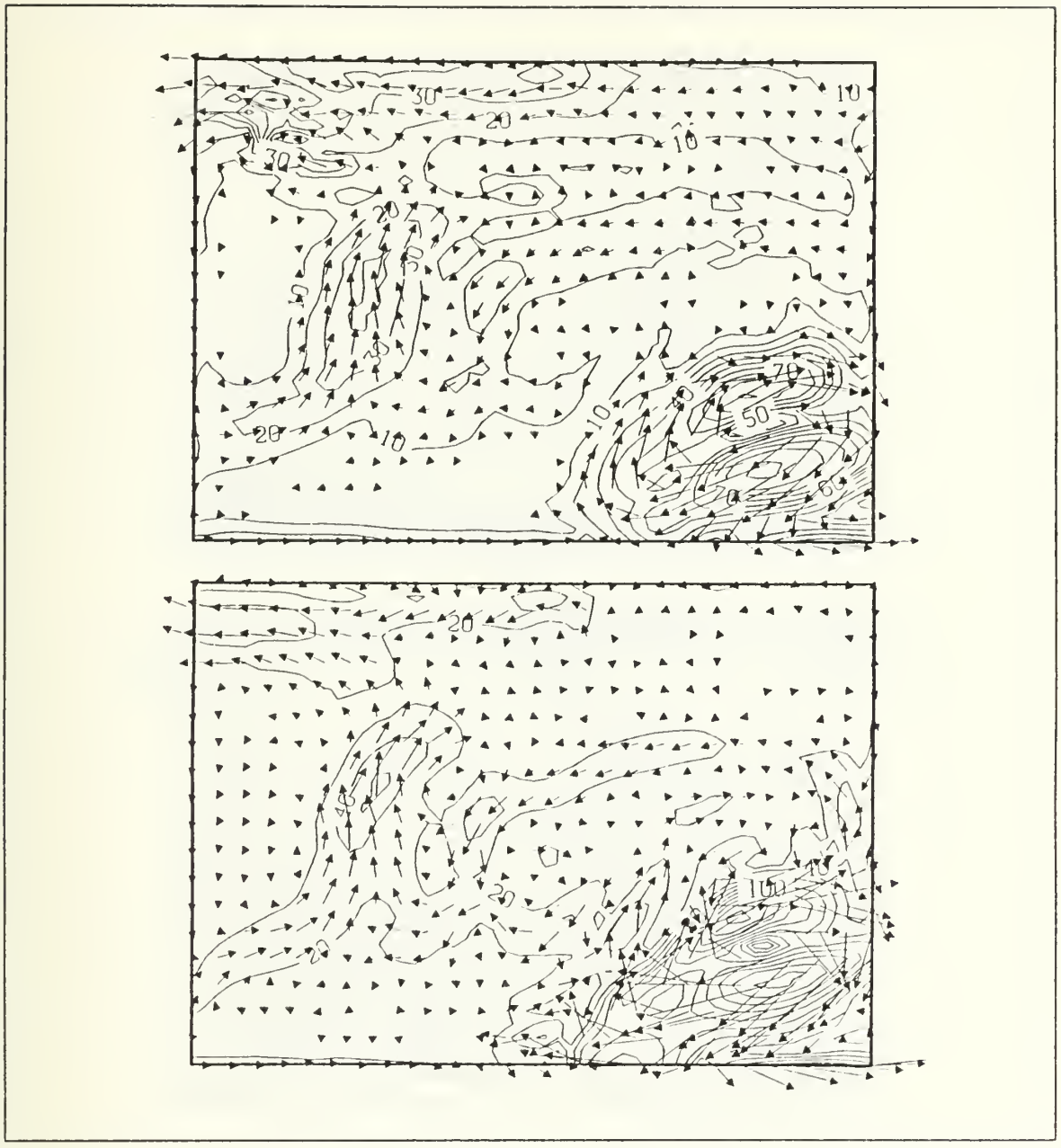

Figure 8. **Experiment No. 4 (Jet Initialization, WSC shear 10/10 cm/sec):** The upper and lower figures represent the upper and lower layer velocity fields respectively for Experiment No. 4. North is to the right in each figure and each figure represents a 522 km by 395 km area. Contour intervals are 10 and 20 cm/sec for the upper and lower layers respectively.

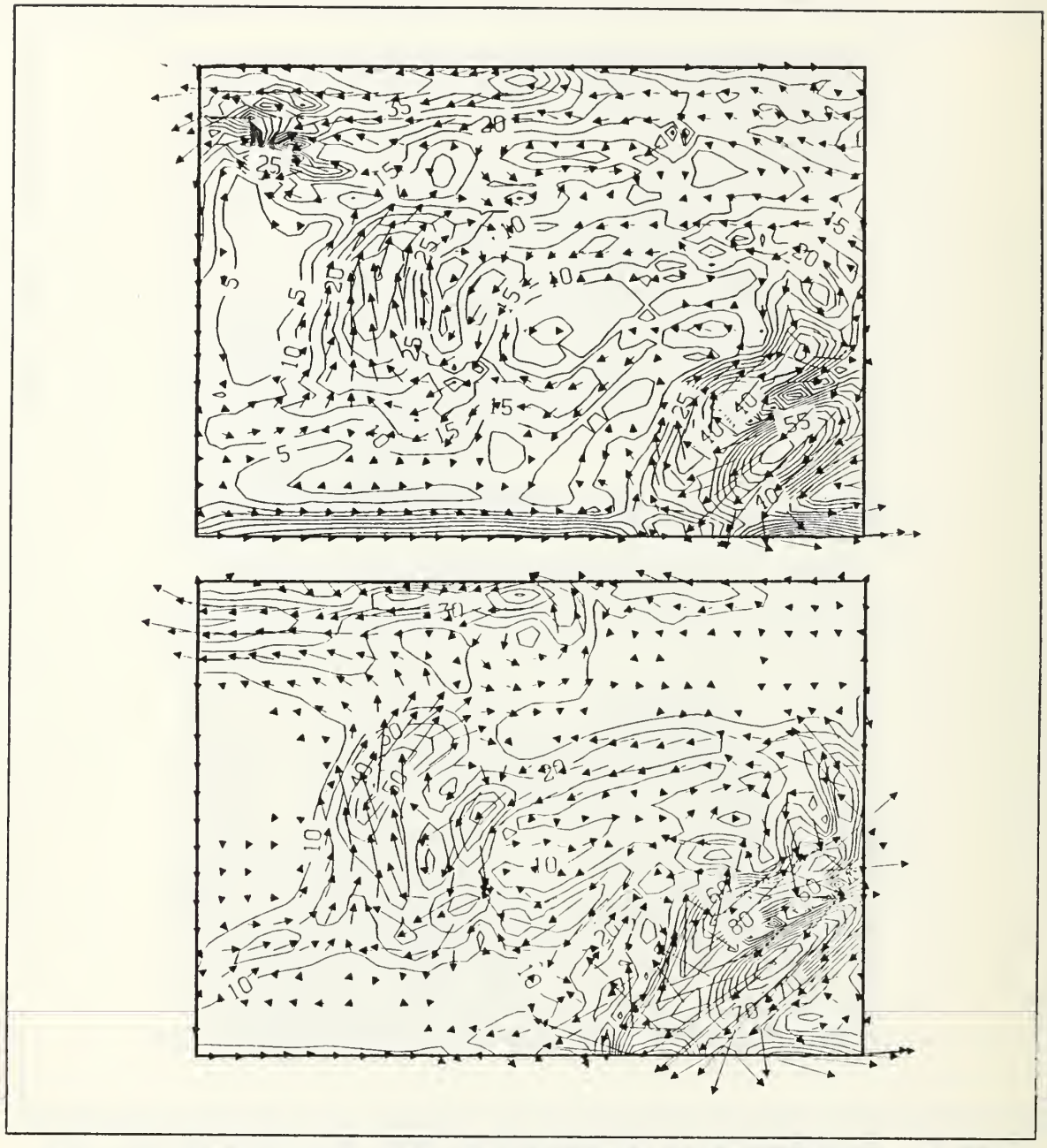

Figure 9. **Experiment No. 5 (Jet Initialization, WSC shear 10/5 cm/sec):** The upper and lower figures represent the upper and lower layer velocity fields respectively for Experiment No. 5. North is to the right in each figure and each figure represents a 522 km by 395 km area. Contour intervals are 5 and 10 cm/sec for the upper and lower layers respectively.

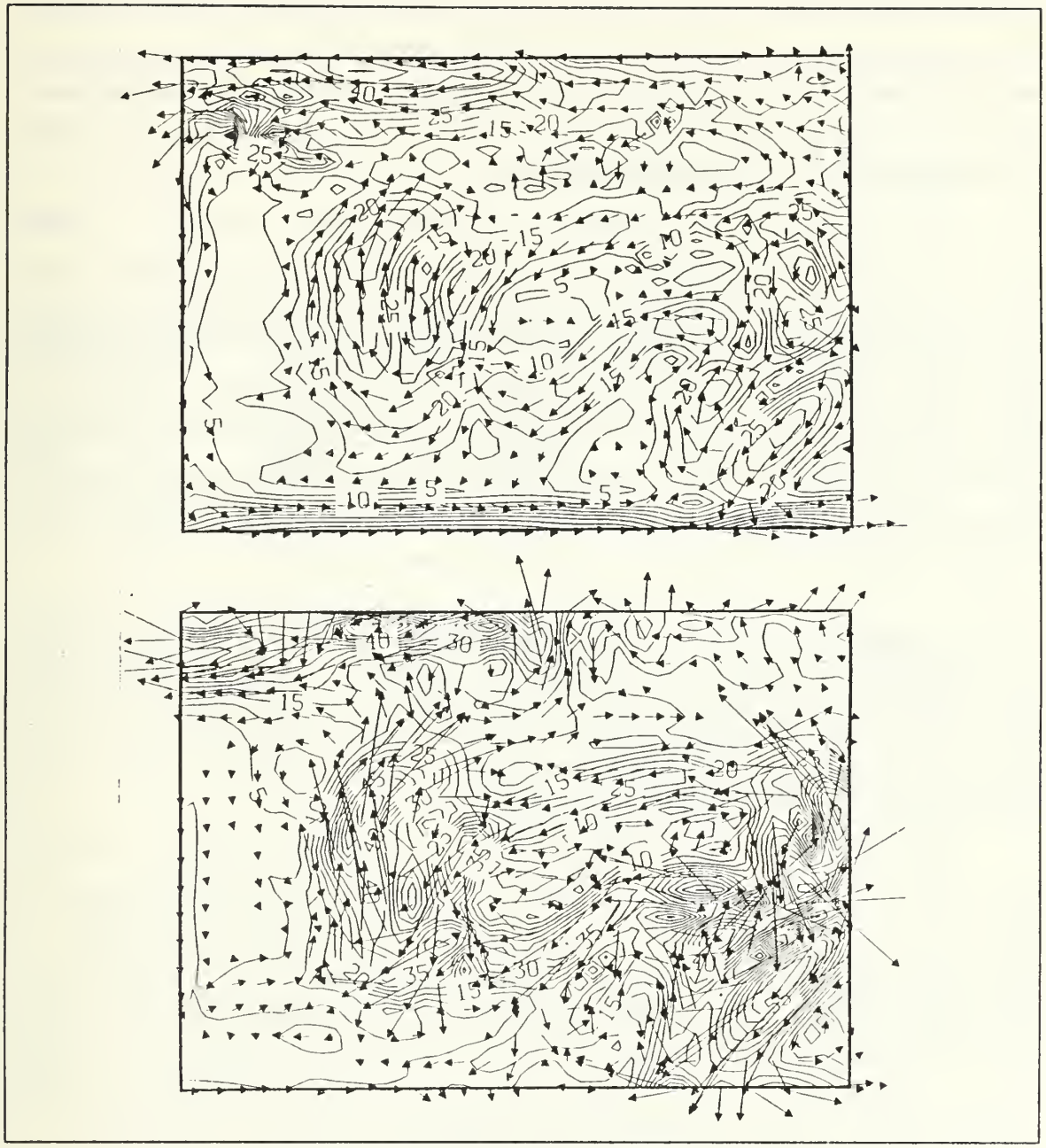

Figure 10. **Experiment No. 6 (Jet Initialization, WSC shear 10/1 cm/sec):** The upper and lower figures represent the upper and lower layer velocity fields respectively for Experiment No. 6. North is to the right in each figure and each figure represents a 522 km by 395 km area. Contour intervals are 5 cm/sec for both the upper and lower layers.

prohibited from following deep isobaths around Yermak plateau by EGC deep flow down Lena trough in the opposite direction. This upslope flow causes vortex squashing over the Yermak plateau and the anticyclonic vortex or vortices is/are produced. Follow-on experiments will investigate methods of removing these vortices, since they are artificially induced by the model constraints.

When Experiments No. 1 through 3 are compared with experiments 4 through 6 it is seen that the model is not particularly sensitive to EGC boundary forcing versus EGC jet initialization with boundary forcing. The most noticeable difference is a broad jet (in the jet initialized experiments) versus a boundary trapped jet (in the boundary forced cases). In jet initialization cases, the lower layer is rapidly eroded by topographic waves. During the early stages of these simulations, these topographic waves naturally arise in the lower layer as a result of forcing with the EGC jet initialization and boundary forcing. These waves have a period of approximately 4 days and wavelengths of approximately 50 km. They propagate along the slope and out the open boundaries within 10 days.

A comparison of experiments 1 through 3 and of experiments 4 through 6 leads to the notion that the existence of the WSC in two branches (one feeding RAC to the west, the other supplying along boundary flow) is dependent upon inflow vertical shear (specifically, 10 5 cm sec in the upper and lower layers respectively was used). No northward branch of WSC is seen in barotropic cases.

During 1985-1986, Fram Strait current measurements were obtained. Current meter measurements from FS-9B were reported by Aagaard *et al.*, (1988) and are included here in table 2. FS-9B data is compared with model current meter data for a model domain location (36, 56) coincident with FS-9B, listed in Table 3. FS-9B is in the RAC region. By sampling the model current velocity in the same location, the ability of the model to correctly simulate RAC is tested. It should be noted that the data at FS-9B was obtained over a record length as indicated in table 2, and the model current velocities are the value on day 10. This necessarily implies that direct comparison cannot be made. However, a qualitative comparison between the two data sets suggests that model output velocities are about twice that of observed. For example, if Experiment No. 3's upper layer current velocity of 22 cm/sec is compared with the value of FS-9B's current meter at 107 meters, a value of 9.9 is seen. The direction of the current sensed at current meter FS-9B is westward, as is that of the model's current. Additionally, the model flow in this region is strongly barotropic despite baroclinic inflow conditions in some simulations. The convergent effect of topography creates enhanced

lower layer flows in this region. Lower layer velocity at this location is not sensitive to the lower layer inflow of WSC indicating that much of the flow there (at least in these runs) originates from deep EGC flow down the Lena trough. A method to reduce the modeled current velocities may be to move the inflow region of the EGC to the west, more up on the slope and thereby reduce the amount of EGC flow down the Lena trough.

Table 2. FRAM STRAIT CURRENT MEASUREMENTS (1985-1986)

Mooring	Instrument depth (meters)	Mean Current (cm/sec)	Record Length (days)
FS-9B	107	9.9	392
FS-9B	407	9.1	287
FS-9B	2532	5.6	392

Table 3. MODEL CURRENT DATA AT 10 DAYS

Experiment	Upper Layer Instantaneous Current (cm/sec)	Lower Layer Instantaneous Current (cm sec)
1	26	28
2	22	26
3	22	22

C. FOLLOW-ON EXPERIMENTS

Follow-on experiments were conducted to address the following issues: can more realistic current flow be obtained at the model position (36, 56)?; is the EGC responsible, at least in part, for the existence of RAC as observed?; and, is the model sensitive to inflow location of the EGC?.

Table 4 lists the follow-on experiments and parameters that were varied. Experiments No. 7 through 9 address the Yermak vortex issue, while Experiment No. 10 is a flat bottom (no topography) case. Experiments No. 11 through 13 address EGC port variation and responsibility for RAC. Experiment No. 13 has modified topography and appears to have many of the features seen in observations. None of the follow-on experiments contained jet initialization. Inflow locations are given in grid point format and the specific locations may be seen in the representative Fram Strait modeled topography for each experiment. The flat bottom (no topography) experiment is included

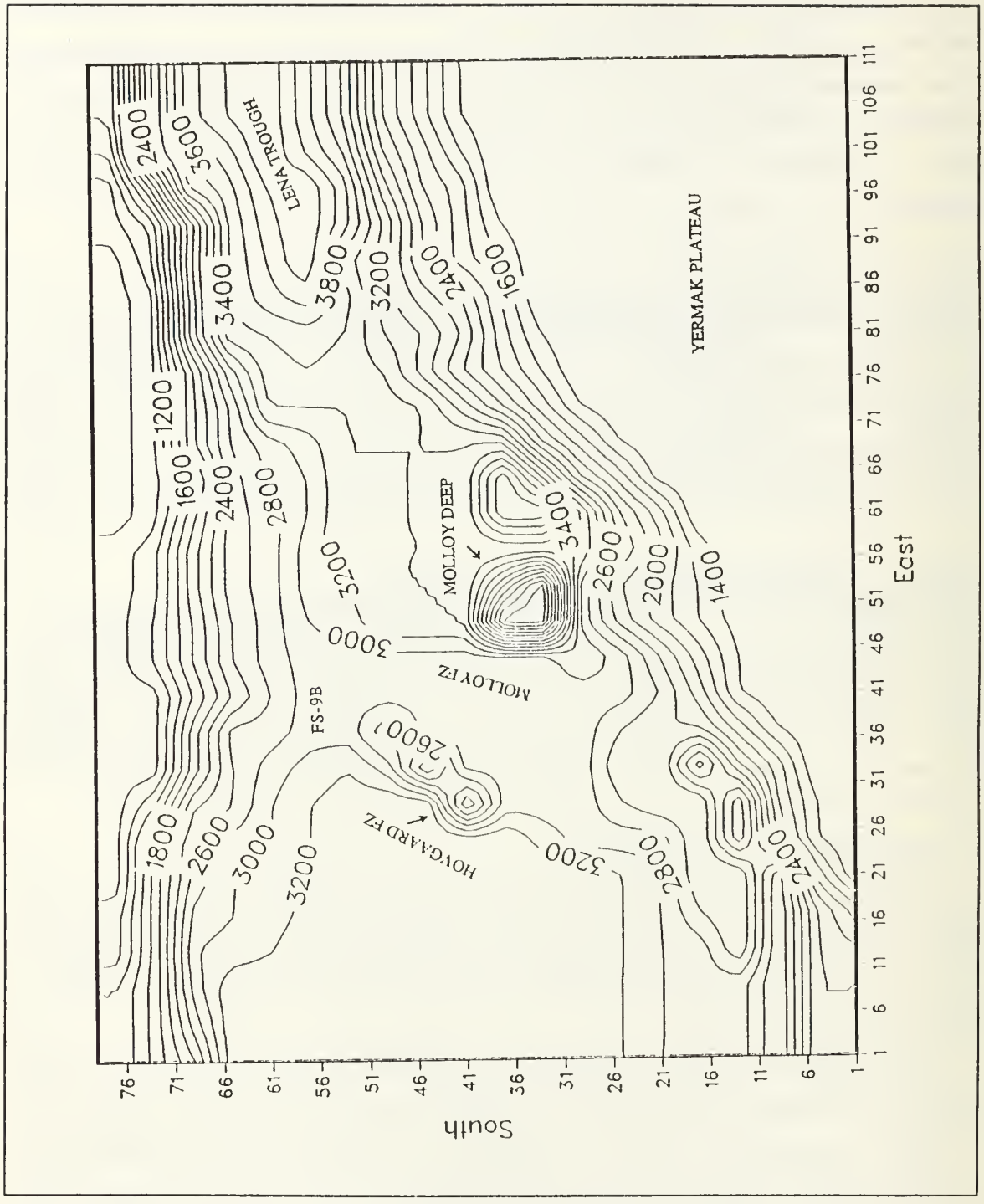

Figure 11. Experiment No. 7: Fram Strait Modified Topography

as an aid in concluding that flows such as the RAC and Yermak anticyclone cannot exist in the absence of topography.

1. **Experiment No. 7 (Topography Modified)**

Experiment No. 7 is boundary forced with a shear of 40/10 cm/sec in the EGC between 55-75, and in the WSC with a 10/5 cm/sec between 5-35. The bottom topography was modified near the eastern boundary such that there were no depths shallower than 1200 meters (see figure 11), thereby moving the Yermak plateau depth to a minimum of 1000 meters below the interface depth. The major difference here is that the large velocity Yermak anticyclone no longer occurs. In the upper layer there is an organized boundary flow along the EGC, RAC exists and appears to be driven by a combination of EGC flow down the Lena trough and WSC flow that has split and has a westward component and a boundary trapped component. In the lower layer there is no EGC boundary current. RAC exists, and WSC boundary current exists but to a lesser degree than in the upper layer. The velocity fields are depicted in figure 12.

Table 4. FOLLOW-ON VARIATION OF MODEL PARAMETERS

Experiment No.	EGC Inflow location	EGC v_1 / v_2 (cm/sec)	WSC Inflow location	WSC v_1 / v_2 (cm sec)	Topography Modified (yes no)
7	55-75	40 10	5-35	10 5	yes
8	55-75	40 10	5-35	10 5	yes
9	55-75	40 10	5-35	10 5	yes
10	65-75	40 10	5-35	10 5	Flat Bottom
11	No Inflow	No Inflow	5-35	10 5	no
12	65-75	40 10	5-35	10 5	no
13	65-75	40 10	5-35	10 5	yes

2. **Experiment No. 8 (Topography Modified)**

As an alternative way of changing the Yermak topography, the 1200 meter isobath was drawn to the northeast corner of the domain (see figure 13) allowing deep outflow all along the northern boundary. The EGC was boundary forced with 40/10 cm sec and the WSC was boundary forced with 10 5 cm sec in the upper and lower layers respectively. In the upper layer, boundary trapped WSC exists. There is no Yermak anticyclone in the upper layer; RAC exists. In the lower layer there is no

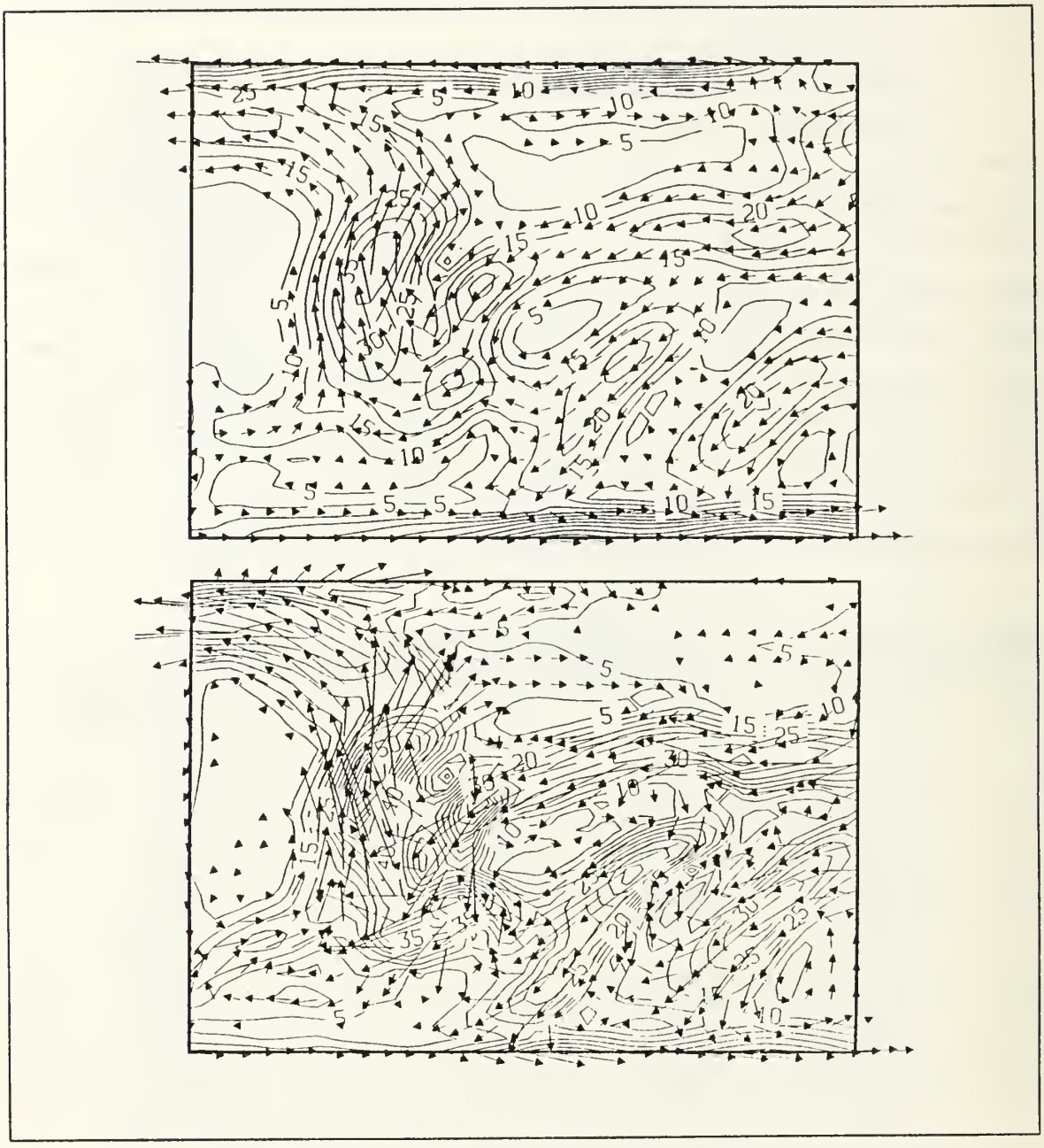

Figure 12. **Experiment No. 7 (Topography Modified):** The upper and lower figures represent the upper and lower layer velocity fields respectively for Experiment No. 7. North is to the right in each figure and each figure represents a 522 km by 395 km area. Contour intervals are 5 cm/sec for both the upper and lower layers.

boundary trapped EGC, there is RAC, and there is no boundary trapped WSC. Although there is no specific Yermak anticyclone, there is a more complex circulation in the east central boundary area of the domain. These motions have strong cross isobath components, indicative of topographic Rossby or continental shelf waves. The velocity fields are depicted in figure 14.

3. Experiment No. 9 (Topography Modified)

In this simulation, the topography was modified (see figure 15) in the area of the WSC inflow such that isobaths were brought parallel to the eastern boundary, thus allowing along isobath inflow, Foldvik (personal communication, 1989). The WSC was boundary forced with 10/5 cm/sec in the upper layer and lower layers respectively. The EGC was boundary forced with 40/10 cm/sec in the upper and lower layers respectively. In the upper layer there is a well organized along boundary EGC, there is RAC fed by WSC and EGC flow down the Lena trough, and there is WSC boundary flow. In the lower layer there is some EGC boundary flow near the exit region, and westward flow (RAC) in the south that appears to be driven by southward flow through the Lena trough. WSC boundary flow exists in both layers. Since the Yermak region was not modified, we see its anticyclone in both he upper and lower layers. The velocity fields are depicted in figure 16.

4. Experiment No. 10 (Flat Bottom)

In this experiment the topography was removed giving a uniform bottom layer thickness of 5400 meters with an upper layer thickness of 200 meters. The EGC was boundary forced with 40/10 cm/sec and the WSC was boundary forced with 10/5 cm/sec in the upper and lower layers respectively. As expected, along boundary flow (east and west) developed in the upper layer and lower layers. The RAC and the Yermak anticyclone are not formed in the absence of topography. The velocity fields are depicted in figure 17.

5. Experiment No. 11 (No EGC)

In this simulation the EGC boundary forcing was eliminated. The WSC was boundary forced with 10/5 cm/sec in the upper and lower layers respectively. The entire northern boundary is open to allow for outflow. In the upper layer there is northward EGC flow, reverse RAC flow and this couples with WSC to flow north through the Lena trough and out the northern boundary. In the lower layer there is similar reverse flow. This demonstrates the need for the EGC to flow southward, thereby causing westward flow of RAC flow as seen in observations of Aagaard *et al.*, (1988). The velocity fields are depicted in figure 18.

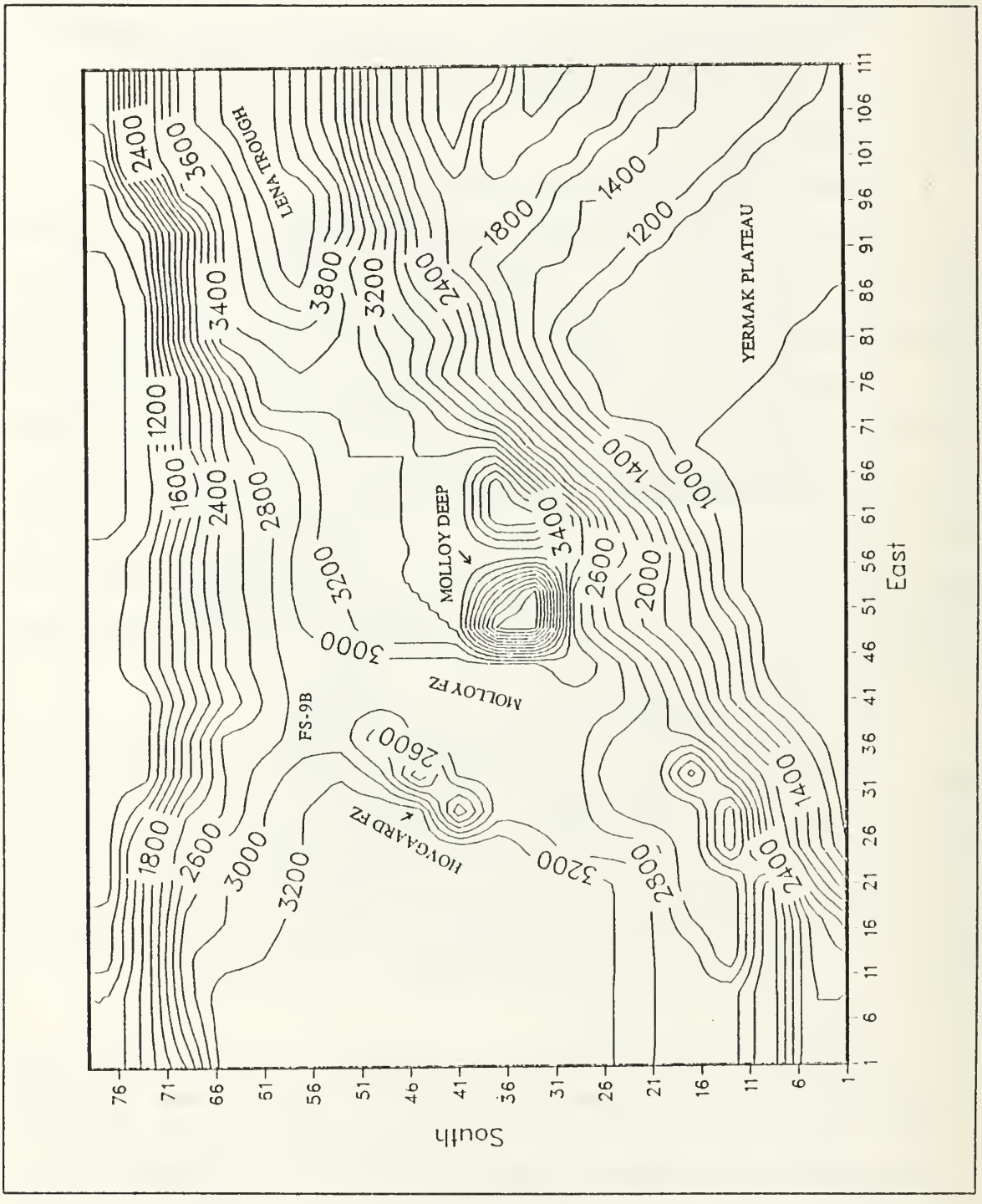

Figure 13. Experiment No. 8: Fram Strait Modified Topography

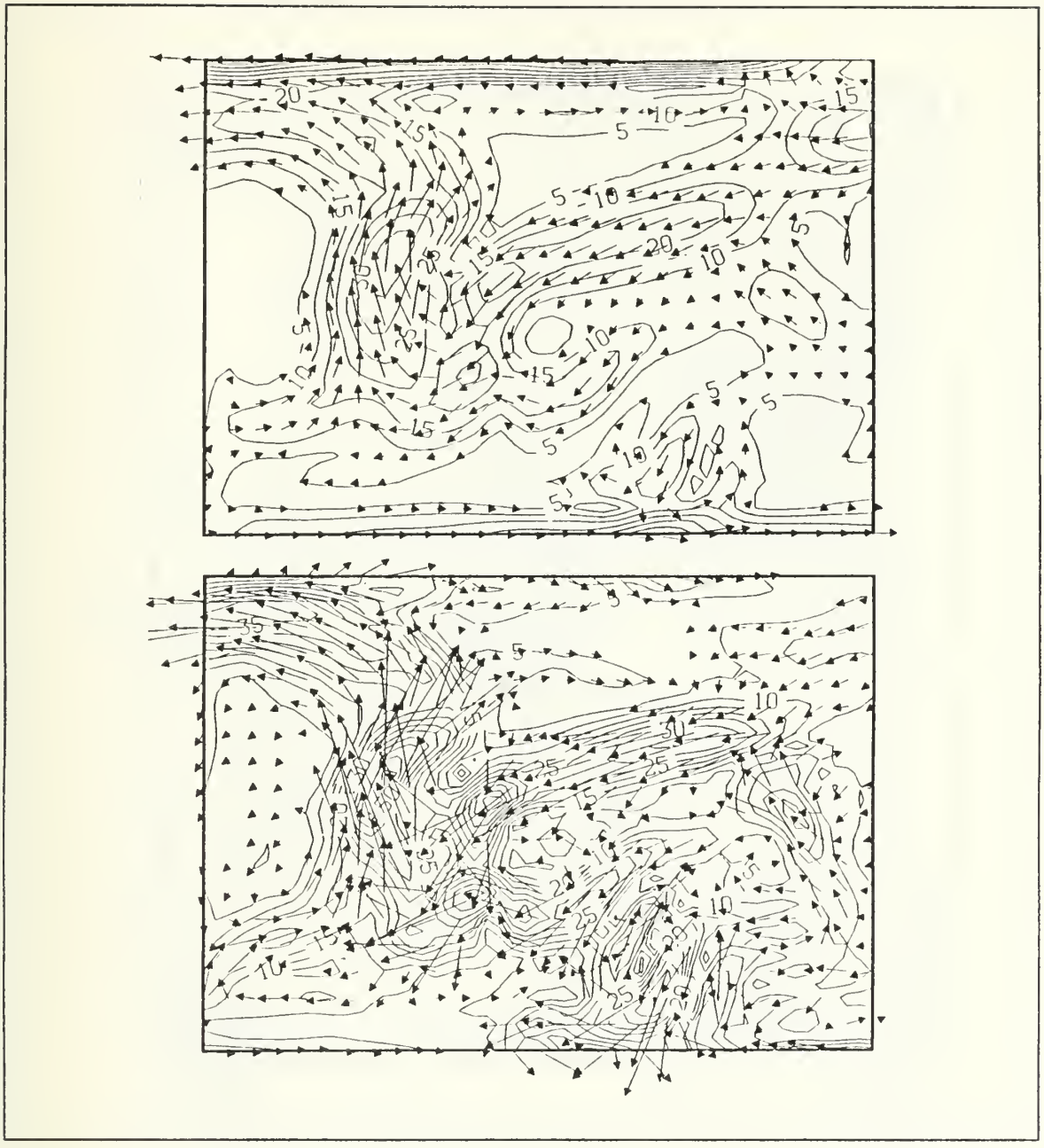

Figure 14. Experiment No. 8 (Topography Modified): The upper and lower figures represent the upper and lower layer velocity fields respectively for Experiment No. 8. North is to the right in each figure and each figure represents a 522 km by 395 km area. Contour intervals are 5 cm/sec for both the upper and lower layers.

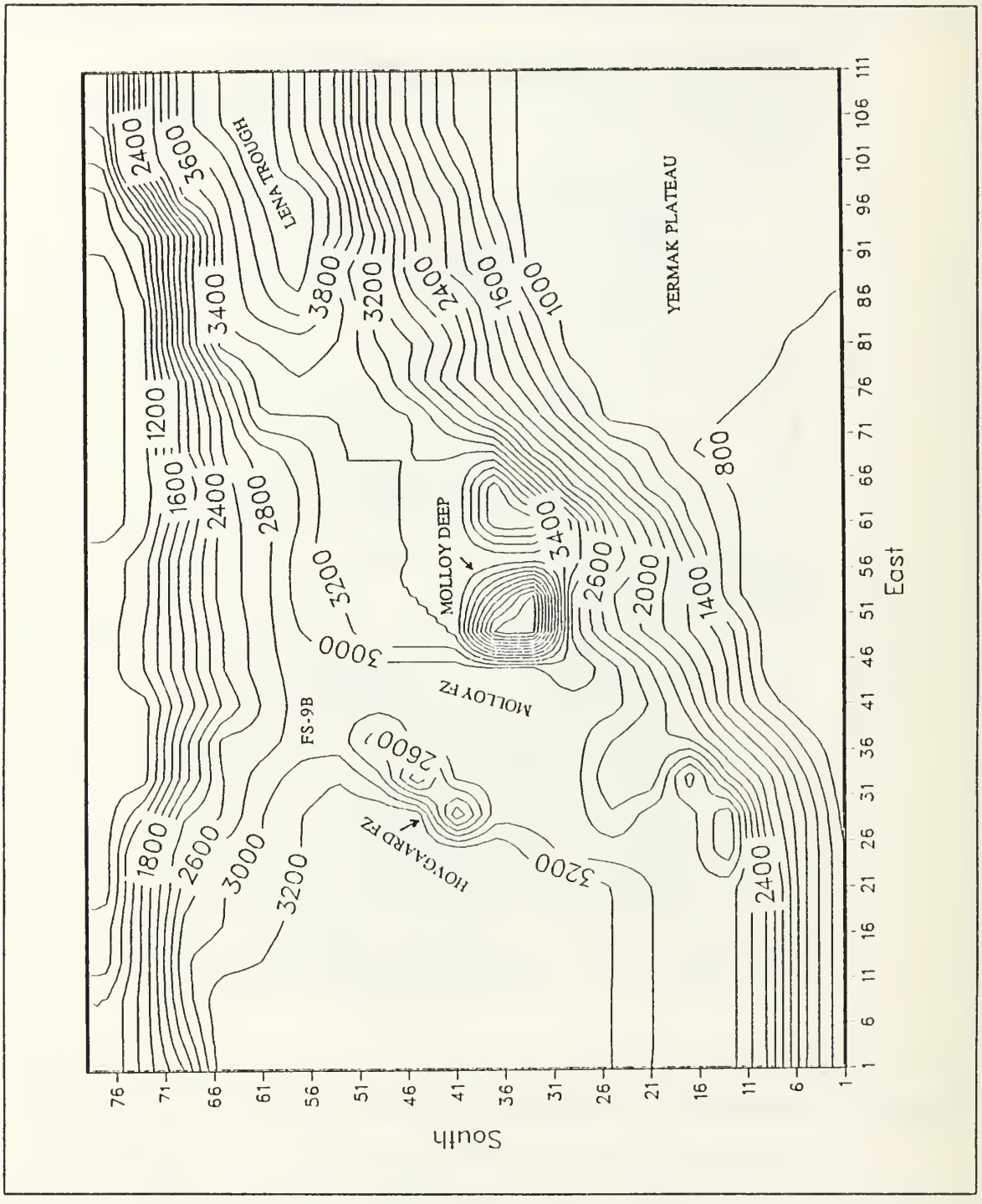

Figure 15. Experiment No. 9: Fram Strait Modified Topography

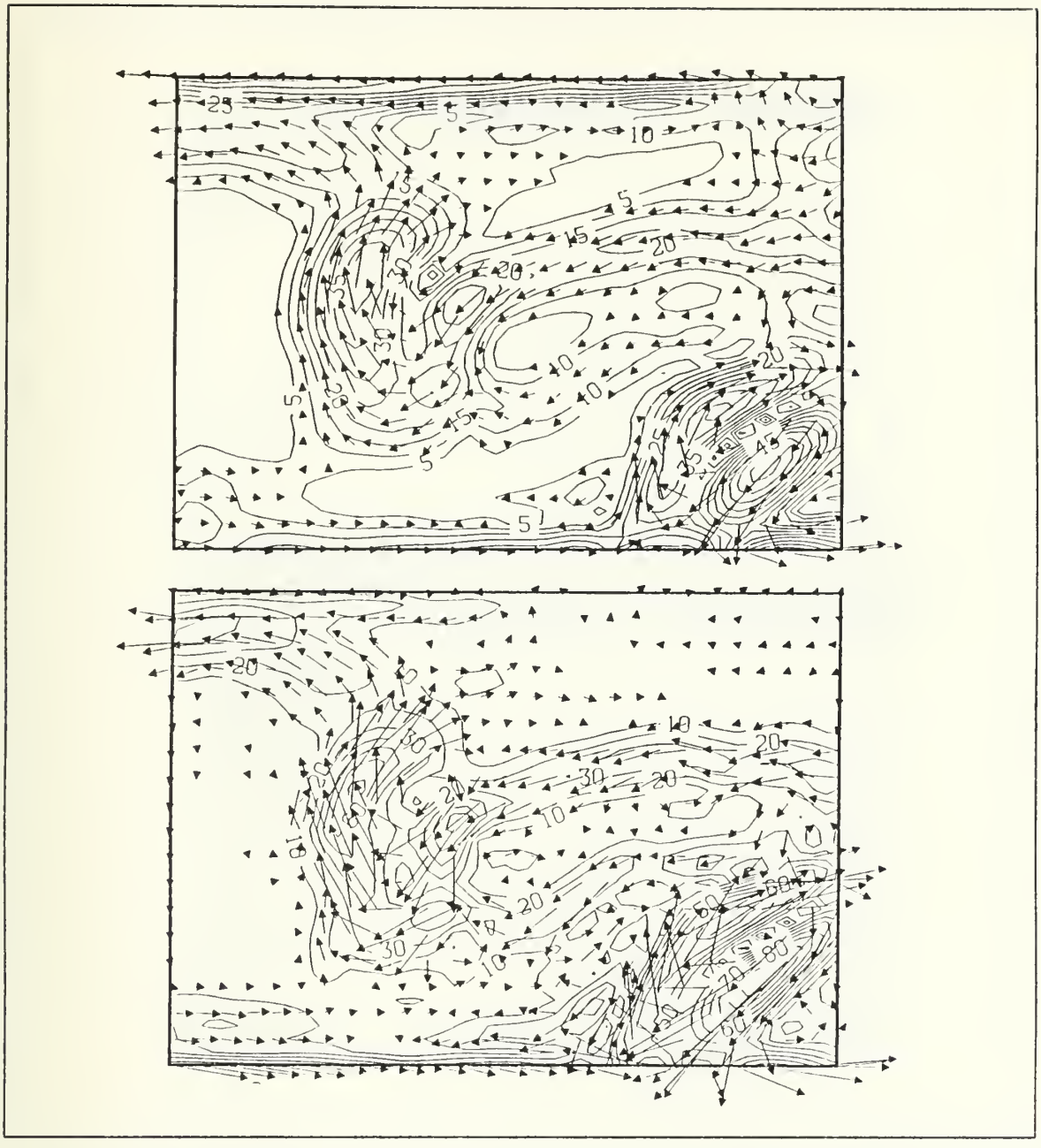

Figure 16. **Experiment No. 9 (Topography Modified):** The upper and lower figures represent the upper and lower layer velocity fields respectively for Experiment No. 9. North is to the right in each figure and each figure represents a 522 km by 395 km area. Contour intervals are 5 and 10 cm/sec for the upper and lower layers respectively.

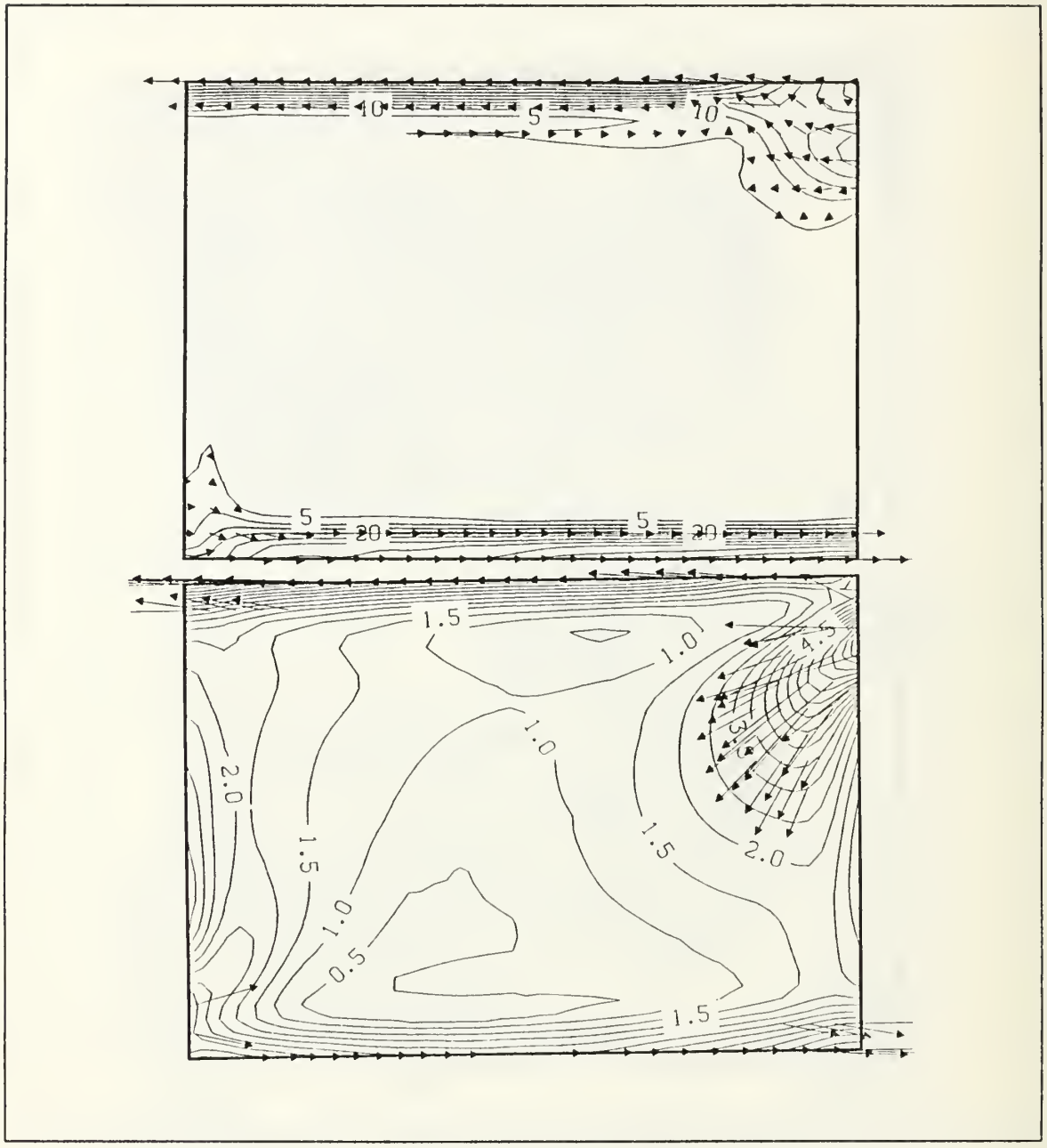

Figure 17. Experiment No. 10 (Flat Bottom): The upper and lower figures represent the upper and lower layer velocity fields respectively for Experiment No. 10. North is to the right in each figure and each figure represents a 522 km by 395 km area. Contour intervals are 5 and .5 cm/sec for the upper and lower layers respectively.

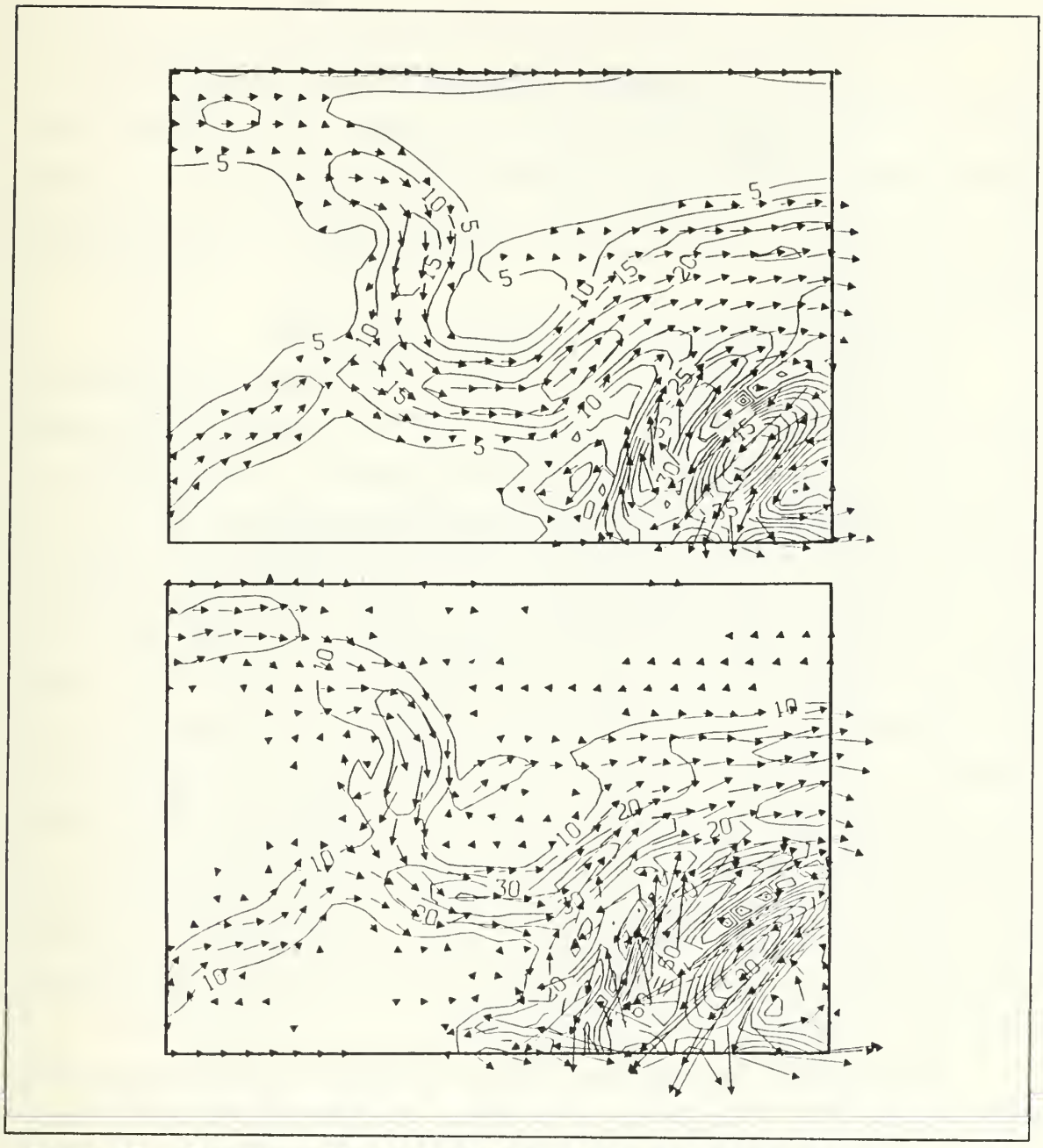

Figure 18. Experiment No. 11 (No EGC): The upper and lower figures represent the upper and lower layer velocity fields respectively for Experiment No. 11. North is to the right in each figure and each figure represents a 522 km by 395 km area. Contour intervals are 5 and 10 cm/sec for the upper and lower layers respectively.

6. Experiment No. 12 (EGC Port Closer to Western Boundary)

In this simulation the EGC was boundary forced with 40/10 cm/sec at 65-75 in the upper and lower layers respectively. The WSC was boundary forced with 10/5 cm/sec at 5-35 in the upper and lower layers respectively. In the upper layer, EGC boundary flow exists, WSC induced RAC exists, and WSC boundary flow exists. Little to no EGC flow is seen in the Lena trough. In the lower layer, WSC induced RAC is seen, and the beginning evolution of boundary trapped EGC is seen. The velocity fields are depicted in figure 19.

7. Experiment No. 13 (Topography Modified, EGC port 65-75)

This experiment was conducted with EGC boundary forcing of 40/10 cm/sec at 65-75 in the upper and lower layers respectively. The WSC was boundary forced with 10/5 cm/sec at 5-35 in the upper and lower layers respectively. The topography was modified (see figure 20) in two areas: first, the WSC inflow region in the south was modified to provide for along isobath flow of the WSC inflow (like that of Experiment No. 9); secondly, the Yermak plateau region was modified by drawing the 1200 meter isobath to the northeast corner as was done in Experiment No. 8. In the upper layer, EGC along boundary flow exists, RAC exists driven by a westward component of the WSC, and weak along boundary WSC is demonstrated. In the lower layer, along isobath flow is seen in the vicinity of the EGC, RAC driven by WSC westward flow is seen, and a northward component of the WSC is seen just east of the Molloy Deep. Northeastward outflow is seen with slight WSC along boundary flow in the south. In the Lena trough, flow is southward on the western side and northward on the eastern side. The northward flow is joined from the south by a northward branch of the WSC that flows northward just east of the Molloy deep area. The velocity fields are depicted in figure 21.

These flow fields are also seen in figure 22 which shows surface and interface height anomaly fields. A comparison of the surface slope field with the corresponding upper ocean velocity vectors indicates that the flow is geostrophically balanced, with flow to the right of the pressure gradient. Interface height anomaly is indicative of the degree of baroclinicity. Largest interfacial slopes (and hence vertical shears) are seen in the EGC region where a downslope of 65 meters in the interface is seen toward the west. The RAC is relatively barotropic.

Although Experiment No. 13 appears to best approximate observed flow directions, it is important to now consider magnitudes of velocities within its domain. For

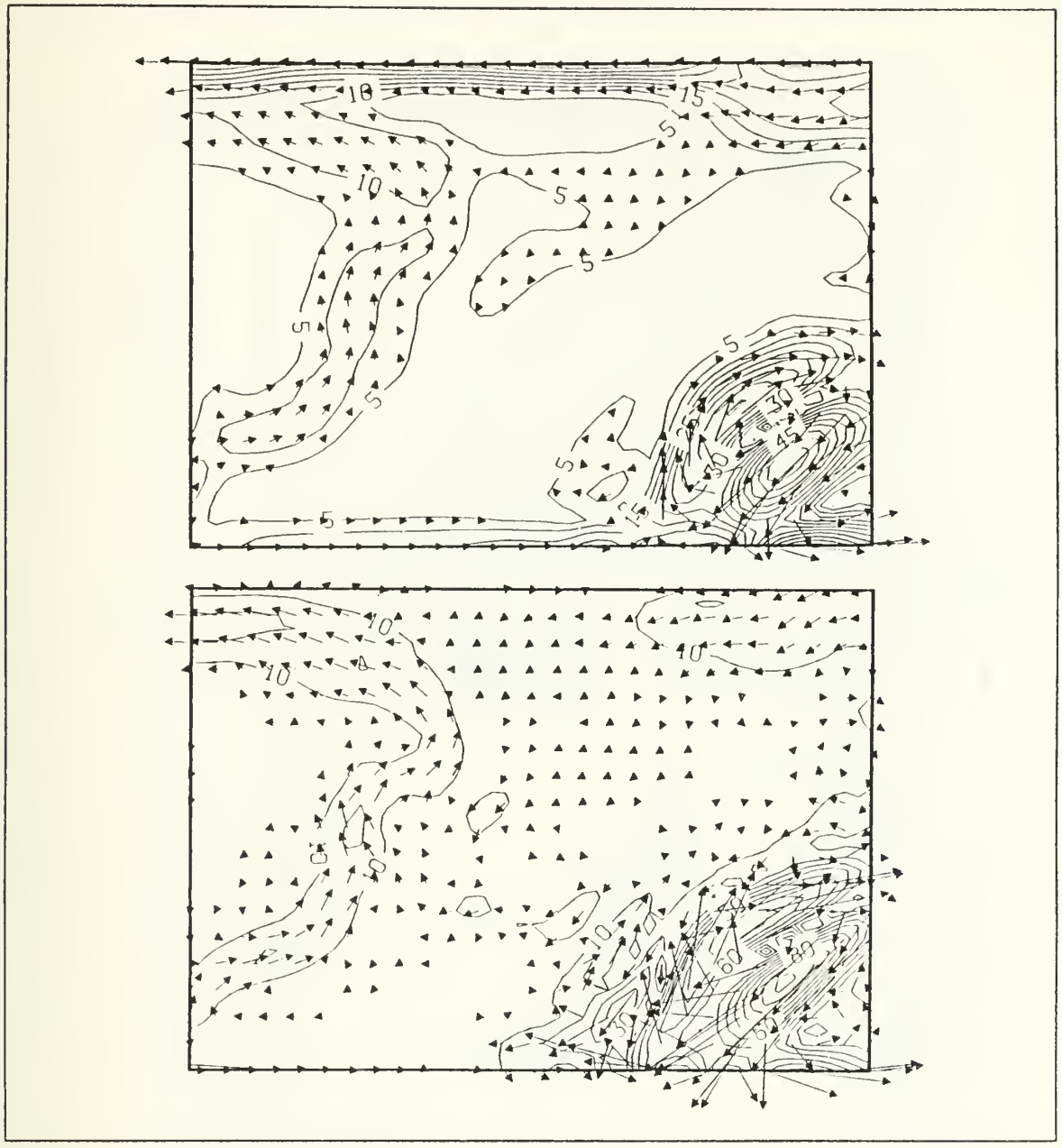

Figure 19. **Experiment No. 12 (EGC Port Closer to Western Boundary):** The upper and lower figures represent the upper and lower layer velocity fields respectively for Experiment No. 12. North is to the right in each figure and each figure represents a 522 km by 395 km area. Contour intervals are 5 and 10 cm/sec for the upper and lower layers respectively.

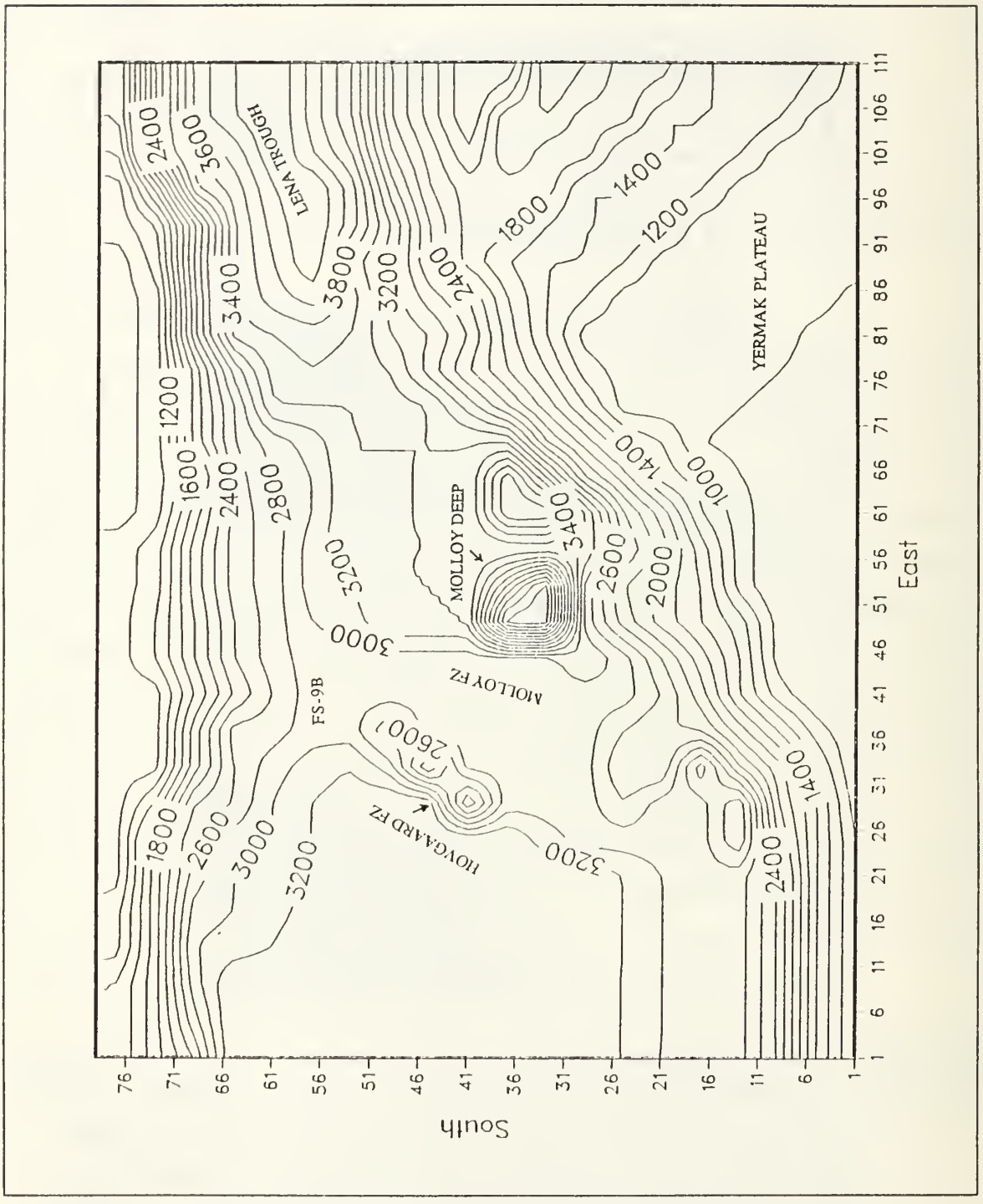

Figure 20. Experiment No. 13: Fram Strait Modified Topography

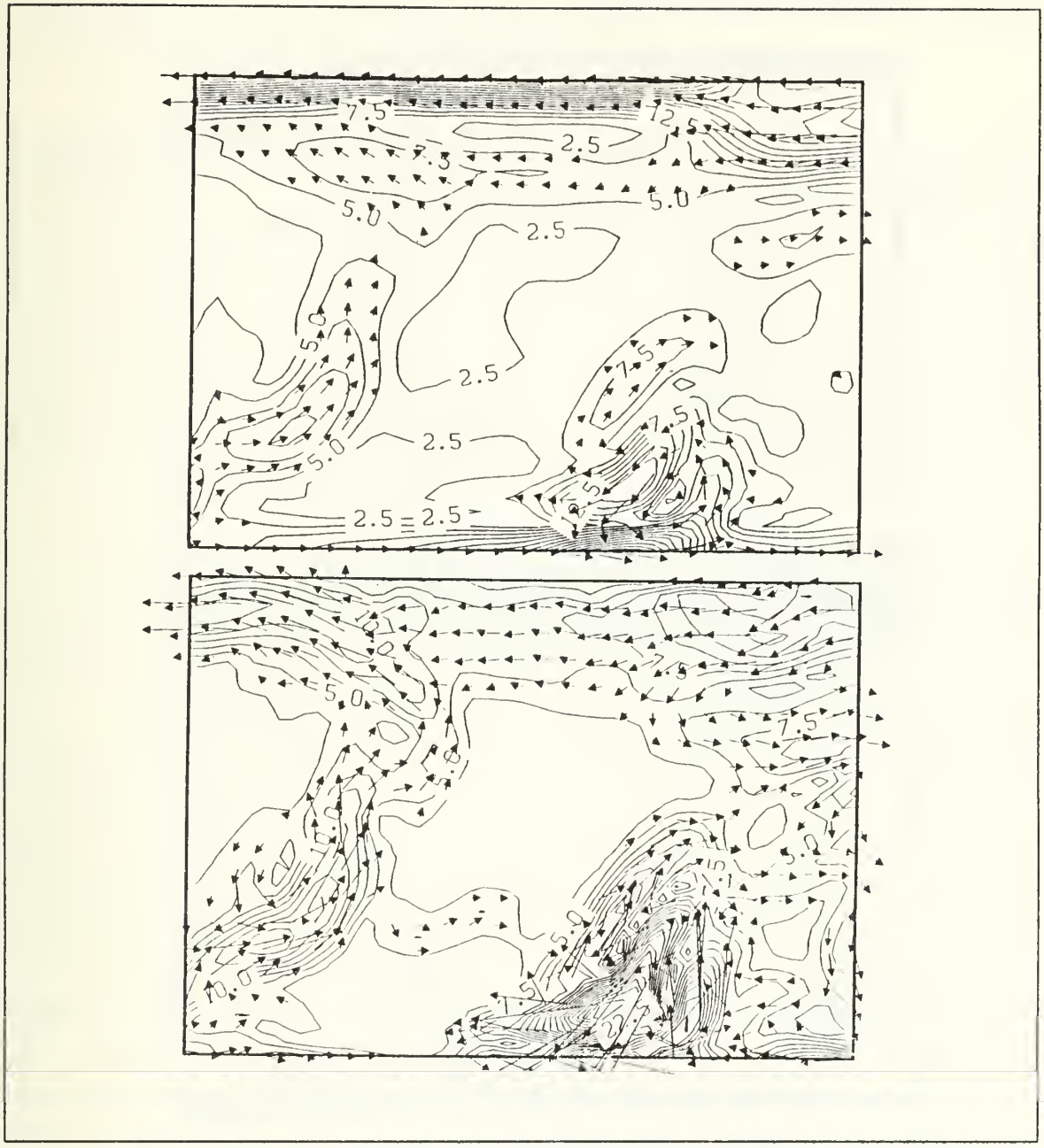

Figure 21. **Experiment No. 13 (Topography Modified, EGC port 65-75):** The upper and lower figures represent the upper and lower layer velocity fields respectively for Experiment No. 13. North is to the right in each figure and each figure represents a 522 km by 395 km area. Contour intervals are 2.5 cm/sec for both the upper and lower layers.

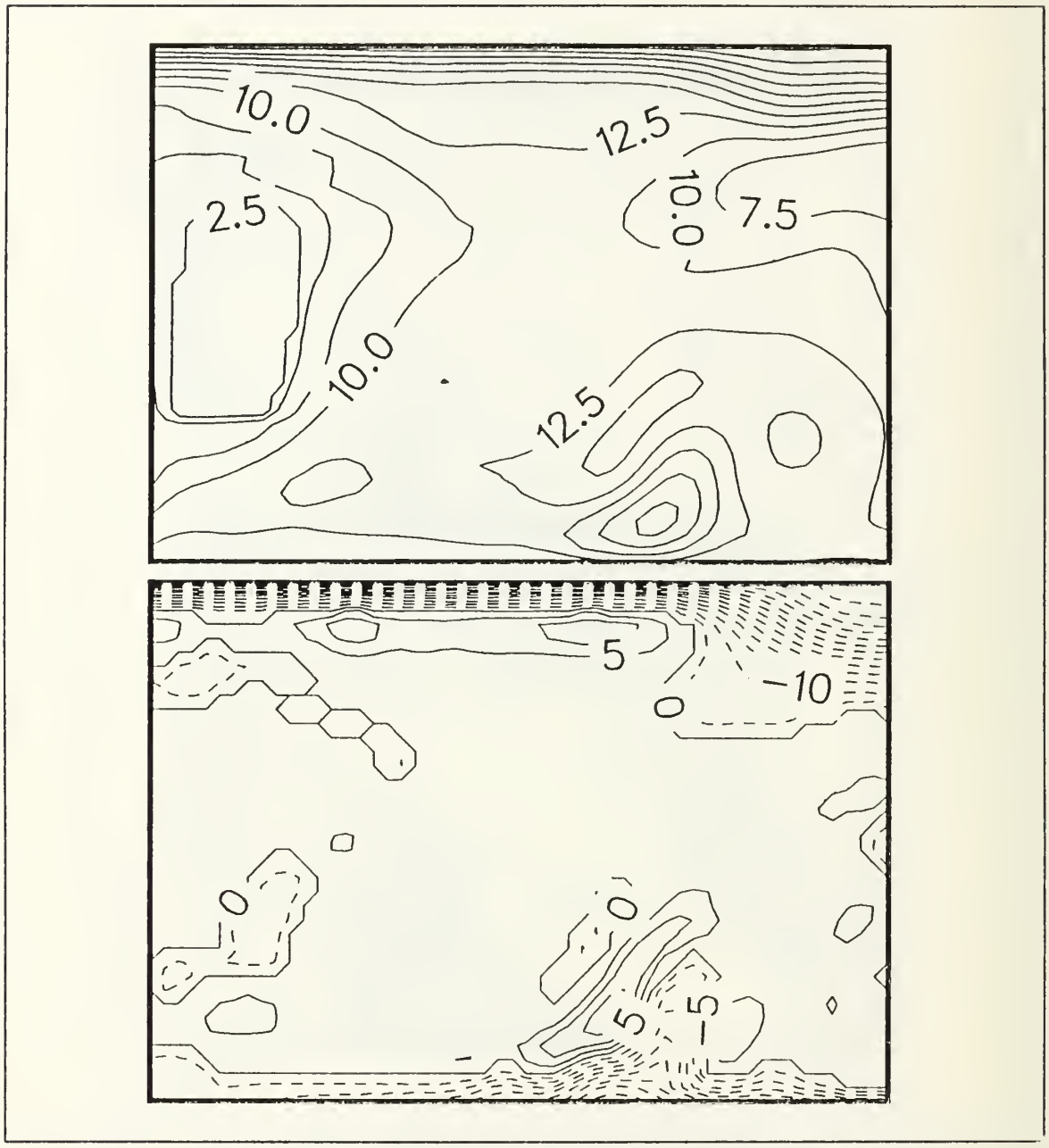

Figure 22. Height Anomaly Fields: The upper field represents the surface height anomaly (Contour Interval = 2.5 cm). The lower field represents the interface height anomaly (Contour Interval = 10 m). Positive (negative) contours represent upward (downward) distortions in the interface.

comparison purposes, table 5 displays model current speeds for selected follow-on experiments versus current meter data from FS-9B presented in table 3.

Table 5. MODEL CURRENT DATA AT 10 DAYS

Experiment No.	Upper Layer Instantaneous Current (cm sec)	Lower Layer Instantaneous Current (cm/sec)
7	27.0	25.0
8	24.0	22.0
9	22.0	22.0
11	23.0	14.0
12	8.5	14.0
13	8.0	11.5

Of particular note is that even for a qualitative comparison, Experiments No. 12 and 13 have velocities close to those obtained at FS-9B, with Experiment No. 13 being very close to the same. This coupled with the flow direction similarity of Experiment No. 13 is suggestive of a correctly modeled Return Atlantic Circulation.

The follow-on experiments indicate a number of more realistic aspects of Fram Strait circulation than do the preliminary experiments. With respect to the RAC, there is reduced magnitude of the flow in Experiments No. 12 and 13 where EGC flow is forced only on the western side of the Lena trough. With respect to the Yermak anticyclone, its absence when shallow isobaths do not extend to the northern boundary (Experiments No. 7, 8 and 13) indicates an improper choice of model domain location relative to isobaths in early simulations. A more appropriate boundary location would follow isobaths. Irregular boundaries are not however allowed with the present model. A shift of the present domain 1° north would allow deep along isobath WSC inflow, and deep along isobath outflow (as seen in Experiment No. 13). In Experiment No. 13, the WSC can realistically split near the Molloy Deep into westward RAC with a small northward flow east of the Molloy Deep. A portion of this flow could then go around the Yermak plateau to the northeast, and a portion could exit to the north via the Lena trough.

IV. CONCLUSIONS AND RECOMMENDATIONS

A. CONCLUSIONS

The Fram Strait with its associated East Greenland Current (EGC), West Spitzbergen Current (WSC), and varied topography is a region of complex circulation and intense dynamical activity. To better understand the topographically steered flows in the Fram Strait will provide one with the ability to better and more effectively employ Naval forces throughout the region and to allow for continued scientific research.

A two layer, semi-implicit, primitive equation, numerical model is used to simulate the general circulation within the Fram Strait. The simulation of the EGC and WSC using boundary forcing provides a more realistic circulation pattern. The model is not particularly sensitive to jet versus no jet initialization. Although the EGC is observed to be jet-like (in the area of the East Greenland Polar Front) in character, from a numerical modeling standpoint jet initialization is not necessary for correct model simulation of the experiments of this study.

The model is sensitive to WSC inflow vertical shear. In simulations with no shear, boundary trapped flows on the eastern and western boundaries could not be produced. When the WSC inflow vertical shear was increased to 10/5 cm/sec, the eastern and western boundary trapped flows were such to cause a reduction in model velocity, and thereby a tendency toward values more in line with those observed by Aagaard *et al*, (1988) at FS-9B. Conversely, if shear is further increased such that upper layer flow is 10 cm/sec and lower layer flow is 1 cm/sec, no appreciable reduction of model current velocity is seen. Therefore, a shear of 10/5 cm/sec appears best to simulate RAC flows.

Varying the port width of the EGC inflow allows for narrow along boundary flow of EGC or if widened a more broad flow extending south through the Lena trough region. By moving the EGC inflow closer to the western boundary, there is a reduction of flow down the Lena trough. This reduced flow down the Lena trough causes a reduction of the model current velocities associated with the RAC region. EGC port forcing on the western side of Lena trough gives more realistic RAC flow values. Unfortunately, no deep current meter measurements in Lena trough are available for comparison with this model.

The EGC is largely responsible for the westward RAC circulation in this model. Although some WSC is required to substantially duplicate observed flow patterns within

the general Fram Strait circulation, the major contributor is the EGC. This is demonstrated by the RAC reversal when EGC is absent.

B. RECOMMENDATIONS

A number of previous studies have indicated the importance of topography in steering ocean flows in the Fram Strait region. This study illustrates the response of topographic steering to flow location and vertical shear of the currents. A number of other effects are however known to be important in the region.

Further studies should incorporate the effects of winds and the marginal ice zone. The existence of an along ice edge wind driven jet could thus be included. Longer simulations including this effect could address instability issues associated with the jet. The effects of mesoscale eddies on the general circulation could then be determined.

In two-layer flows over topography, the upper layer may respond too strongly to topographic steering of the lower layer. This effect could be determined in future studies by the incorporation of a third model layer.

In this study, inflow port locations were the same for upper and lower layer flows. The effect of forcing upper and lower flows at different locations should be addressed in future studies. Specifically, a broad upper layer East Greenland Current forced over a narrow deep inflow west of the Lena Trough may give more realistic results.

V. APPENDIX- SYMBOLS AND NOTATION

B_h	Biharmonic friction coefficient	$= 5.0 \times 10^{10}\ m^4/s$
A_S, A_I	Initial surface and interfacial height anomaly of the jet	
f_0	Coriolis parameter for mean latitude 80°N	
g	Gravitational acceleration	
g'	Reduced gravitational acceleration	$= g(\rho_2 - \rho_1)/\rho_1 = .02\ m/s^2$
h_i	Instantaneous upper (i = 1) and lower (i = 2) layer thickness	
H_i	Upper (i = 1) and lower (i = 2) layer mean thickness	
i,j	Grid indices in x,y directions	= 111,79
L_j	e-folding scale for the jet	= 20 km
p_1	Pressure in the upper layer	$= g(h_1 + h_2 + d)$
p_2	Pressure in the lower layer	$= p_1 - g'h_1$
Q_i	Potential vorticity $(f + \zeta_i) / h_i$	
R_d	First internal Rossby radius of deformation	
	$= 1/f\sqrt{(g'H_1H_2)/(H_1 + H_2)}$	= 13.7 km
R_0	Rossby number	$= v_{max}/(fL)$
u_i, v_i	Velocities in the x and y directions	
U_i, V_i	Transport in the x and y directions	
v_{max}	Maximum jet velocity	
x,y	Cartesian coordinates directed E and N respectively	
Δx	Delta x	= 4.7 km
Δy	Delta y	= 5.0 km
Δt	Model time step	= 2400 sec
ρ_i	Density in i^{th} layer	
∇	Gradient operator	$= \partial/\partial x + \partial/\partial y$
∇^2	Laplacian operator	$= \partial^2/\partial x^2 + \partial^2/\partial x^2$
ζ_i	Upper (i = 1), lower (i = 2) layer relative vorticity	
	$= \partial v_i/\partial x - \partial u_i/\partial y$	
y_0	Eastern edge of the jet	

VI. LIST OF REFERENCES

Aagaard, K., 1982: Inflow from the Atlantic Ocean to the polar basin. *The Hydrographic Environment and the Fate of Pollutants*, edited by Louis Rey, pp. 69-82.

_____, C. Darnall, A. Foldvik, M. Steg, and T. Torresen, 1988: Fram Strait current measurements, 1985-1986. *Rep.* 66, 43 pp., Univ. of Bergen, Bergen, Norway, (Also published as *Rep.* 1091, Univ. of Washington, Seattle).

Bourke, R. H., M. D. Tunnicliffe, J. L. Newton, R. G. Paquette, and T. O. Manley, 1987: Eddy near the Molloy Deep revisited, *J. Geophys. Res.*, **92(C7)**, 6773-6776.

_____, A.M. Weigel and R.G. Paquette, 1988: The westward turning branch of the West Spitzbergen Current. *J. Geophys. Res.*, **93**, 14,065-14,077.

Camerlengo, A. L., and J. J. O'Brien, 1980: Open boundary conditions in rotating fluids, *J. Comput. Phys.*, **35**, 12-35.

Foldvik, A., K. Aagaard and R. Torresen, 1988: On the velocity field of the East Greenland Current. *Deep-Sea Research*, **35**, 1335-1354.

Gascard, J.C., C. Kergomard, P.F. Jeannin and M. Fily, 1988: Diagnostic study of the Fram Strait marginal ice zone during summer from 1983 and 1984 marginal ice zone experiment Lagrangian observations. *J. Geophys. Res.*, **93**, 3613-3641.

Hanzlick, D. J., 1983: The West Spitzbergen Current, transport, forcing, and variability. Ph. D. Thesis, Univ. of Wash., Seattle, 127 pp.

Hurlburt, H.E., 1974: The influence of coastline geometry and bottom topography on the eastern ocean circulation. Ph. D. thesis, Florida State University, 103 pp.

_____, and J.D. Thompson, 1980: A numerical study of loop current intrusions and eddy shedding. *J. Geophys. Res.*, **9**, 1611-1651.

_____, and _____, 1982: The dynamics of the loop current and shed eddies in a numerical model of the Gulf of Mexico. *Hydrodynamics of Semi-Enclosed Seas*, Elsvier, 243-298.

Johannessen, O.M., J.A. Johannessen, J. Morison, B.A. Farrelly and E.A.S. Svendsen, 1983: Oceanographic conditions in the marginal ice zone north of Svalbard in early fall 1979 with an emphasis on mesoscale processes. *J. Geophys. Res.*, **88**, 2755-2769.

Paquette, R.G., R.H. Bourke, J.F. Newton and W.F. Perdue, 1985: The East Greenland Polar Front in autumn. *J. Geophys. Res.*, **90**, 4866-4882.

Quadfasel, F., J.G. Gascard and K.P. Koltermann, 1987: Large-scale oceanography in Fram Strait during the 1984 marginal ice zone experiment. *J. Geophys. Res.*, **90,** 6719-6728.

Smith, D.C. IV, and J.J. O'Brien, 1983: The interaction of a two-layer isolated mesoscale eddy with topography. *J. Phys. Oceanogr.*, **13,** 1681-1697.

_____, and G. P. Davis, 1989: A numerical study of eddy interaction with an ocean jet. *J. Phys. Oceanogr.***19**, 975-986.

_____, and R.O. Reid, 1982: A numerical study of nonfrictional decay of mesoscale eddies. *J. Phys. Oceanogr.*, **12,** 244-255.

VII. INITIAL DISTRIBUTION LIST

		No. Copies
1.	Defense Technical Information Center Cameron Station Alexandria, VA 22304-6145	2
2.	Library, Code 0142 Naval Postgraduate School Monterey, CA 93943-5002	2
3.	Chairman (Code 63Rd) Department of Meteorology Naval Postgraduate School Monterey, CA 93943-5000	1
4.	Chairman (Code 68Co) Department of Oceanography Naval Postgraduate School Monterey, CA 93943-5000	1
5.	Professor D. C. Smith IV (Code 68Si) Department of Oceanography Naval Postgraduate School Monterey, CA 93943-5000	3
6.	Professor Arne Foldvik (Code 68Fv) Department of Oceanography Naval Postgraduate School Monterey, CA 93943-5000	1
7.	Professor J. C. Gascard (Code 68Ga) Department of Oceanography Naval Postgraduate School Monterey, CA 93943-5000	1
8.	Director Naval Oceanography Division Naval Observatory 34th and Massachusetts Avenue NW Washington, DC 20390	1
9.	Commander Naval Oceanography Command Naval Oceanography Command NSTL Station Bay St. Louis, MS 39522	1
10.	Commanding Officer Fleet Numerical Oceanography Center Monterey, CA 93943	1

11.	Commanding Officer Naval Oceanographic Office NSTL Station Bay St. Louis, MS 39522	1
12.	Commanding Officer Naval Ocean Research and Development Activity NSTL Station Bay St. Louis, MS 39522	1
13.	Commanding Officer Naval Environmental Prediction Research Facility Monterey, CA 93943	1
14.	Chairman, Oceanography Department U. S. Naval Academy Annapolis, MD 21402	1
15.	Chief of Naval Research 800 North Quincy Street Arlington, VA 22217	1
16.	Office of Naval Research (Code 420) Naval Ocean Research and Development Activity 800 North Quincy Street Arlington, VA 22217	1
17.	Commanding Officer Polar Oceanography Center, Suitland Washington, DC 20373	1
18.	LCDR David W. McShane 1114 Spruance Road Monterey, CA 93940	2

Thesis
M26977 McShane
c.1 A numerical study of topographically steered flows in the Fram Strait.

5 MAY 87 37402

Thesis
M26977 McShane
c.1 A numerical study of topographically steered flows in the Fram Strait.

thesM26977
A numerical study of topographically ste
3 2768 000 82448 6
DUDLEY KNOX LIBRARY
C.1